NATIONAL ADVISORY COMMITTEE FOR AERONAUTICS

TECHNICAL NOTE

No. 1010

STRESS-STRAIN AND ELONGATION GRAPHS FOR ALUMINUM ALLOY R301 SHEET

By James A. Miller
National Bureau of Standards

Washington
February 1946

NATIONAL ADVISORY COMMITTEE FOR AERONAUTICS

TECHNICAL NOTE NO. 1010

STRESS-STRAIN AND ELONGATION GRAPHS FOR ALUMINUM ALLOY R301 SHEET

By James A. Miller

SUMMARY

The following properties were determined from tests on duplicate longitudinal and transverse specimens from aluminum alloy R301 sheets with nominal thicknesses of 0.020, 0.032, and 0.064 inch:

Tensile and compressive stress-strain graphs and stress-deviation graphs of sheet in the T condition to a strain of about 1 percent

Graphs of tangent modulus and of reduced modulus for a rectangular section versus strain in compression of sheet in the T condition

Tensile stress-strain graphs to failure of sheet in the W condition and in the T condition

Local elongation and elongation versus gage length for tensile specimens from sheet in the W condition and in the T condition tested to fracture

The stress-strain, stress-deviation, tangent-modulus, and reduced-modulus graphs are plotted on a dimensionless basis to make the results of a limited number of tests applicable to materials with similar stress-strain curves and with yield strengths which differ from those of the test specimens. An example is given to illustrate how these graphs may be used.

INTRODUCTION

This report is the first of a series presenting data obtained on high-strength aluminum alloy sheet. The data

are assembled in the form of tables and graphs similar to those presented for steels and for earlier aluminum alloys in reference 1 and for a magnesium alloy in reference 2. The graphs are presented in dimensionless form to make them applicable to specimens of these materials with yield strengths which differ from those of the test specimens. The scope of the data has been extended as compared with references 1 and 2 to include tensile stress-strain curves to failure and curves of elongation as a function of gage length. The tensile stress-strain curves to failure are useful for computation of spring-back after forming; they also indicate to some degree the ability of the material to absorb energy before rupture. The local elongation data were included because of their usefulness in computing minimum bend radii for forming operations. (See reference 3.) All data are given for duplicate specimens.

The report gives the results of tests on aluminum alloy R301 sheet, in thicknesses of 0.020, 0.032, and 0.064 inch, supplied by Reynolds Metals Company.

The dimensionless graphs were derived from data obtained in tests for the Bureau of Aeronautics, Navy Department. The permission of the Bureau of Aeronautics for the use of these data is gratefully acknowledged. The author also expresses his appreciation to Mr. P. L. Peach and Mrs. P. V. Jacobs, who assisted in the testing and in the preparation of the graphs.

This investigation, conducted at the National Bureau of Standards, was sponsored by and conducted with the financial assistance of the National Advisory Committee for Aeronautics.

MATERIAL

The sheets were of Reynolds aluminum alloy R301 in the "W" (quenched) condition and in the "T" (artificially aged) condition as furnished by the manufacturer. This alloy is normally supplied in the cladded form. The percentage of cladding on each side varies with thickness as follows: 10 percent for sheet up to 0.024 inch thick, 7.5 percent for sheet 0.025 to 0.040 inch thick, 5 percent for sheet 0.041 to 0.102 inch thick and 2.5 percent for thicker sheet. Tests were made on sheets nominally 0.020, 0.032, and 0.064 inch thick which were taken to represent sheet with cladding on each side amounting to 10, 7.5, and 5 percent, respectively, of the sheet thickness.

DIMENSIONLESS GRAPHS

Test Procedure

Tensile tests were made on two longitudinal (in direction of rolling) specimens and on two transverse (across direction of rolling) specimens for each thickness of sheet in the T condition. The specimens corresponded to type 5 specimens described in reference 4.

The specimens were tested in a beam-and-poise, screw-type, testing machine of 50-kip capacity using the 5-kip range. They were held in Templin grips. The strain was measured with a pair of Tuckerman 1-inch optical strain gages attached to opposite sheet-faces of the reduced section. The rate of loading was about 2 ksi per minute.

Compressive tests were made on two longitudinal and two transverse specimens from each sheet. The specimens were rectangular strips 0.50 inch wide by 2.25 inches long.

The compressive specimens were tested between hardened steel bearing blocks in the subpress described in reference 5, in the testing machine used for the tensile tests. Lateral support against premature buckling was furnished by lubricated solid guides as described in reference 6. The strain was measured with a pair of Tuckerman 1-inch optical strain gages attached to opposite edge-faces of the specimen. The rate of loading was about 2 ksi per minute.

Test Results

The results of the tensile and compressive tests are given in table 1. Each value of Young's modulus in the table was taken as the slope of a least-square straight line fitted to the lower part of the stress-strain curve. The yield strengths, offset method, were obtained from the stress-strain curves and the experimental values of Young's modulus. The yield strengths, secant method (0.7 E) and (0.85 E), were obtained from the stress-strain curves and values of secant modulus, respectively, 0.7 and 0.85 times the experimental values of Young's modulus.

Stress-Strain Graphs

The stress-strain graphs are plotted in dimensionless form in figures 1, 2, 8, 9, 15, and 16. The coordinates σ, ϵ in these graphs are defined by

$$\sigma = \frac{s}{s_1} \qquad \epsilon = \frac{E_e}{s_1}$$

where

s stress corresponding to strain e

s_1 0.7 E secant yield strength

E Young's modulus

Stress-Deviation Graphs

Dimensionless stress-deviation graphs are shown in figures 3, 4, 10, 11, 17, and 18. The ordinates are the same as for the stress-strain graphs. The abscissas are the corresponding values of $\delta = \epsilon - \sigma$. All the curves intersect at the point $\delta = 1$, $\delta = 3/7$, which corresponds to the 0.7 E secant yield strength. This point is indicated on the graphs by a short vertical line.

The graphs were plotted on log-log paper to indicate which portion of the stress-strain curves can be represented by the analytical expression

$$e = \frac{s}{E} + K\left(\frac{s}{E}\right)^n$$

given in reference 7. This relationship holds where the plot of deviation against stress on log-log paper is a straight line, for

$$\log\left(e - \frac{s}{E}\right) = \log K + n \log \frac{s}{E}$$

or

$$\log (\epsilon - \sigma) = \log K \left(\frac{s_1}{E}\right)^{n-1} + n \log \sigma$$

The graphs indicate that the relationship holds for the compressive specimens and for the longitudinal tensile specimens, for values of $s/s_1 > s_2/s_1$, where s_2 is the 0.85 E secant yield strength. For these, the ratios s_1/s_2, given in table 1,

can be used to obtain values of the shape parameter n as shown in reference 7. Other straight lines can be drawn on these graphs from which values of k and n can be obtained for analytical expressions which fit more closely other parts of the stress–strain graphs.

Tangent–Modulus–Strain Graphs

Dimensionless tangent–modulus–strain graphs are shown in figures 5, 6, 12, 13, 19, and 20. The ordinates are the ratios of tangent modulus E' to Young's modulus. Each value of tangent modulus was taken as the ratio of a stress increment to its strain increment. The abscissas were the mean values of ϵ for the strain increments. Only a few values of tangent modulus were computed at the upper end of the range used for the Young's modulus determination.

The graphs show no evidence of a secondary modulus.

Reduced–Modulus–Strain Graphs

Dimensionless reduced–modulus–strain graphs are shown in figures 7, 14, and 21. The ordinates are the ratios of reduced modulus for a rectangular cross section E_r to Young's modulus, and the abscissas are the corresponding values of ϵ. The curves were derived from the corresponding tangent–modulus–strain curves using the formula:

$$\frac{E_r}{E} = \frac{4E'/E}{\left(1 + \sqrt{E'/E}\right)^2}$$

TENSILE STRESS–STRAIN GRAPHS TO FAILURE

Tensile tests to failure were made on two longitudinal and two transverse specimens from sheets of each thickness in both the W and T conditions. The specimens corresponded to type 5 specimens described in reference 4.

The tests were made in fluid–support, Bourdon–tube hydraulic testing machines having Tate–Emery load indicators. The specimens were held in Templin grips. They were tested at a cross–head speed of about 0.1 inch per minute. Autographic load–extension curves were obtained with a Templin

type stress-strain recorder using a Peters total elongation extensometer with a 2-inch gage length and a magnification factor of 20.

Stresses based on the original cross section and the corresponding strains based on the original gage length were determined from these curves. The data for the portion at and beyond the knee of each curve were combined with corresponding stress-strain data on duplicate specimens on which strain had been measured with Tuckerman optical strain gages.

The resulting stress-strain curves are shown in figures 34 to 36. Values of tensile strength and elongation in 2 inches are given in the tables accompanying each figure. The values of elongation usually corresponded to a strain of about 0.006 less than the maximum recorded strain under load.

LOCAL ELONGATION GRAPHS

Procedure

Photogrid measurements (reference 8) were made on two longitudinal and two transverse tensile specimens from sheets of each thickness in both the W and T conditions. The specimens corresponded to type 5 specimens described in reference 4.

A grid was photographed on one side of each specimen. The negative was made from a master grid ruled at the National Bureau of Standards. The grid spacing was 0.250 millimeter (approx. 0.01 in.). The width of the lines was about 0.015 millimeter. A survey of a photographic negative obtained from the master grid indicated that the spacing of lines was constant within ±0.003 millimeter or within ±1.2 percent. In the middle region where readings on the specimen were taken at each line, the spacing was constant within ±1 percent. A survey of the photogrid on a specimen indicated that the constancy of spacing was of the same order.

Some of the specimens were coated with photoengraving glue, but most of them were coated with cold top enamel. The latter seemed to be less critical to exposure time and gave prints which were usually easier to measure near the fracture than were the prints obtained with the glue.

The specimens were held in Templin grips and were fractured in a testing machine at a cross-head speed of about 0.1 inch per minute.

Measurements of grid spacing along a longitudinal line were made on the fractured specimens. In order to obtain accurate measurements at the fracture a line was chosen which was crossed by the fracture as nearly at right angles as possible in the middle third of the spacing between two adjacent lines. Where the fracture was intersected by a region in which noticeable necking had taken place, the line was chosen to pass through the intersection. Usually the line was near the middle of the specimen; it was in no case less than 0.11 inch from an edge.

The measurements of grid spacing were made with a Zeiss measuring microscope at a magnification of 56 diameters. The instrument was read to 0.001 millimeter (0.1 division on the barrel).

The specimen was alined parallel with the micrometer screw of the microscope. Readings were taken along the selected line at the edges of the fracture, at each intersection for about 20 spaces each side of the fracture and from there on at intervals of, at most, 10 spaces to the ends of the gage length. At least two readings were made at each place. At the fracture and throughout the region of appreciable necking duplicate readings were made by two independent observers. The nominal spacing before application of load was subtracted from the lengths thus determined to obtain the local elongations.

Local Elongation Graphs

The local elongations, in percent of the original spacing, plotted against the distance before test from one end of the gage length, are shown in figures 23, 24, 26, 28, 30, and 32.

The fracture in each case occurred in the grid spacing in which the greatest elongation took place.

Elongation versus Gage Length Graphs

The elongations in percent of the original gage length were computed for various gage lengths from the local elongation data. These values are plotted against gage length in

figures 23, 25, 27, 29, 31, and 33. The gage lengths were plotted to a logarithmic scale to present a large range of values on a single graph.

DISCUSSION

The dimensionless stress-strain graphs for specimens taken in the same direction in the sheet and for the same kind of loading fell within narrow bands (figs. 37 and 38), even though the various sheets differed in percentage of cladding and differed in yield strength up to $5\frac{1}{2}$ percent. The maximum width of band in terms of σ was 0.013 in tension and 0.022 in compression. While part of this spread may be attributed to experimental variations, most of it was due to differences in shape between the graphs for the various sheets. Stress-strain graphs of the same shape, or linearly affine stress-strain graphs, should form a common curve when plotted as σ versus ϵ.

The limits within which the curves shown in the compressive tangent-modulus-strain graphs (figs. 5, 6, 12, 13, 19, and 20) fell are shown in figure 39: similar graphs for reduced modulus for a rectangular section are shown in figure 40. The maximum spread in values of E'/E or of E_r/E for any of the bands was 0.064.

It should be noted that each set of maximum and minimum values shown is based on tests of 6 specimens. It is likely that tests on a much larger number of specimens would give stress-strain graphs differing sufficiently from these in shape to cause the bands to be somewhat wider.

The graphs of figures 37 to 40 are useful for estimating values of stress, strain, tangent modulus, and reduced modulus, for R301-T sheet between 0.020 and 0.064 inch in thickness, for which Young's modulus and the secant yield strength in the desired direction are given. This is illustrated in detail by the following example.

EXAMPLE

Given 0.051 inch R301-T sheet with a Young's modulus

for longitudinal tension $E = 10{,}500$ ksi

for longitudinal compression $E = 10{,}750$ ksi

and with a 0.7 E secant yield strength

for longitudinal tension $s_1 = 62.0$ ksi

for longitudinal compression $s_1 = 61.5$ ksi

Estimate longitudinal tensile and compressive strain and longitudinal tangent modulus and reduced modulus in compression for a stress $s = 55$ ksi.

The stress $s = 55$ ksi corresponds to values of σ:

Longitudinal tension $\sigma = s/s_1 = 55.0/62.0 = 0.887$

Longitudinal compression $\sigma = s/s_1 = 55.0/61.5 = 0.894$

The corresponding values of ϵ should lie inside the horizontally hatched bands of figures 37 and 38. This gives

	σ	ϵ_{min}	ϵ_{max}	ϵ_{av}
Longitudinal tension	0.887	0.940	0.946	0.943
Longitudinal compression	.894	.970	1.015	.992

The strains are related to ϵ by

Longitudinal tension $e = s_1\epsilon/E = 62.0\epsilon/10500 = 0.00590\epsilon$

Longitudinal compression $e = s_1\epsilon/E = 61.5\epsilon/10750 = 0.00572\epsilon$

Substituting the above values of ϵ in these relations gives

	e_{min}	e_{max}	e_{av}
Longitudinal tension	0.00555	0.00558	0.00556
Longitudinal compression	.00555	.00580	.00567

The tangent modulus and reduced modulus ratios are given by the horizontally hatched bands in figures 39 and 40. With the above average value of ϵ:

	ϵ	$(E'/E)_{min}$	$(E'/E)_{max}$	$(E'/E)_{av}$
Longitudinal compression	0.992	0.42	0.47	0.45

	ϵ	$(E_r/E)_{min}$	$(E_r/E)_{max}$	$(E_r/E)_{av}$
Longitudinal compression	0.992	0.62	0,66	0.64

The estimated values of tangent modulus and of reduced modulus are obtained by multiplying the above ratios by E = 10,750 ksi. This gives:

	s	$(E')_{min}$	$(E')_{max}$	$(E')_{av}$
Longitudinal compression	55	4500	5100	4900 ksi

	s	$(E_r)_{min}$	$(E_r)_{max}$	$(E_r)_{av}$
Longitudinal compression	55	6700	7100	6900 ksi

National Bureau of Standards,
Washington, D. C., June 1, 1945.

REFERENCES

1. Aitchison, C. S., and Miller, James A.: Tensile and Pack Compressive Tests of Some Sheets of Aluminum Alloy, 1025 Carbon Steel, and Chromium-Nickel Steel. NACA TN No. 840, 1942.

2. Aitchison, C. S., and Miller, James A.: Tensile and Compressive Tests of Magnesium Alloy J-1 Sheet. NACA TN No. 913, 1943.

3. Gerard, George: Determining Bend Radius - Via Analytical Approach. Aviation, March 1945, pp. 152-156.

4. Anon.: General Specification for Inspection of Metals, Federal Specification QQ-M-151a, Federal Standard Stock Catalog, sec. IV, pt. 5, Nov. 27, 1936.

5. Aitchison, C. S., and Miller, James A.: A Subpress for Compressive Tests. NACA TN No. 912, 1943.

6. Miller, James A.: A Fixture for Compressive Tests of Thin Sheet Metal between Lubricated Steel Guides. NACA TN No. 1022 (to be published).

7. Ramberg, Walter, and Osgood, William R.: Description of Stress-Strain Curves by Three Parameters. NACA TN No. 902, 1943.

8. Brewer, Given A., and Glassco, Robert B.: Determination of Strain Distribution by the Photo-grid Process. Jour. Aero. Sci., vol. 9, no. 1, Nov. 1941, pp. 1-7.

Table 1. Results of tensile and compressive tests on aluminum alloy R301-T sheet.

Spec. No.	Test	Direction	Thickness	Young's modulus E	Yield strength			s_1/s_2	Tensile strength	Elongation in 2 in.
					offset method (offset = 0.2%)	secant method				
						s_1 (0.7E)	s_2 (0.85E)			
			in.	kips/in.^{2}	kips/in.^{2}	kips/in.^{2}	kips/in.^{2}		kips/in.^{2}	percent
16-T1L	Tensile	Longitudinal	0.0198	10,500	60.8	61.1	59.5	1.028	67.8	9.5
16-T2L	"	"	.0198	10,490	60.5	60.8	59.1	1.029	67.5	9.0
16-T1T	"	Transverse	.0197	10,490	58.3	58.8	55.2	1.066	66.4	10.5
16-T2T	"	"	.0198	10,560	58.3	58.9	55.0	1.072	66.1	10.0
16-C1L	Compressive	Longitudinal	.0197	10,780	60.6	61.4	57.3	1.072	-	-
16-C2L	"	"	.0198	10,770	60.4	61.2	57.2	1.070	-	-
16-C1T	"	Transverse	.0197	10,730	62.3	62.9	60.2	1.045	-	-
16-C2T	"	"	.0197	10,750	62.2	62.8	60.2	1.043	-	-
18-T1L	Tensile	Longitudinal	.0311	10,540	63.4	63.8	62.1	1.028	70.9	10.5
18-T2L	"	"	.0311	10,490	63.0	63.4	61.5	1.031	70.8	10.0
18-T1T	"	Transverse	.0312	10,470	60.6	61.4	57.7	1.065	69.2	11.0
18-T2T	"	"	.0311	10,480	60.2	61.0	57.1	1.068	69.3	10.5
18-C1L	Compressive	Longitudinal	.0311	10,750	63.2	64.6	59.4	1.087	-	-
18-C2L	"	"	.0311	10,740	63.2	64.5	59.3	1.087	-	-
18-C1T	"	Transverse	.0312	10,770	64.9	65.9	62.6	1.053	-	-
18-C2T	"	"	.0312	10,790	64.6	65.5	62.4	1.050	-	-
9-T3L	Tensile	Longitudinal	.0630	10,520	62.3	62.6	61.2	1.024	68.8	11.0
9-T2L	"	"	.0630	10,560	62.5	62.8	61.4	1.024	68.8	11.0
9-T1T	"	Transverse	.0630	10,640	59.8	60.4	56.9	1.062	68.3	10.5
9-T2T	"	"	.0632	10,590	60.4	60.9	57.5	1.059	68.7	10.5
9-C1L	Compressive	Longitudinal	.0631	10,790	61.4	62.1	58.7	1.057	-	-
9-C2L	"	"	.0631	10,800	61.5	62.2	58.8	1.057	-	-
9-C1T	"	Transverse	.0632	10,870	64.5	65.1	62.7	1.038	-	-
9-C2T	"	"	.0630	10,820	63.8	64.4	62.0	1.038	-	-

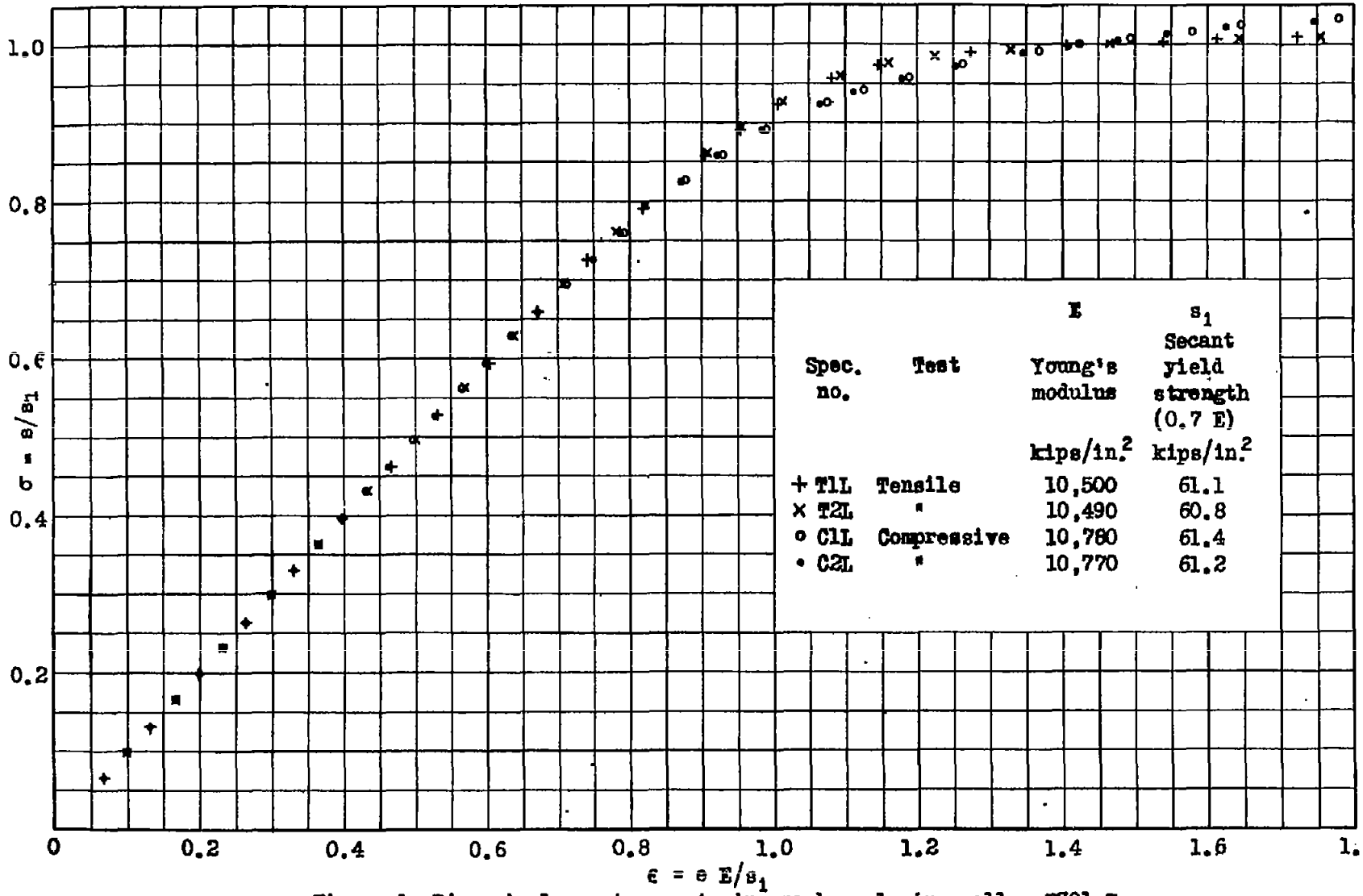

Figure 1. Dimensionless stress-strain graphs, aluminum alloy R301-T, longitudinal specimens 0.020 in. thick.

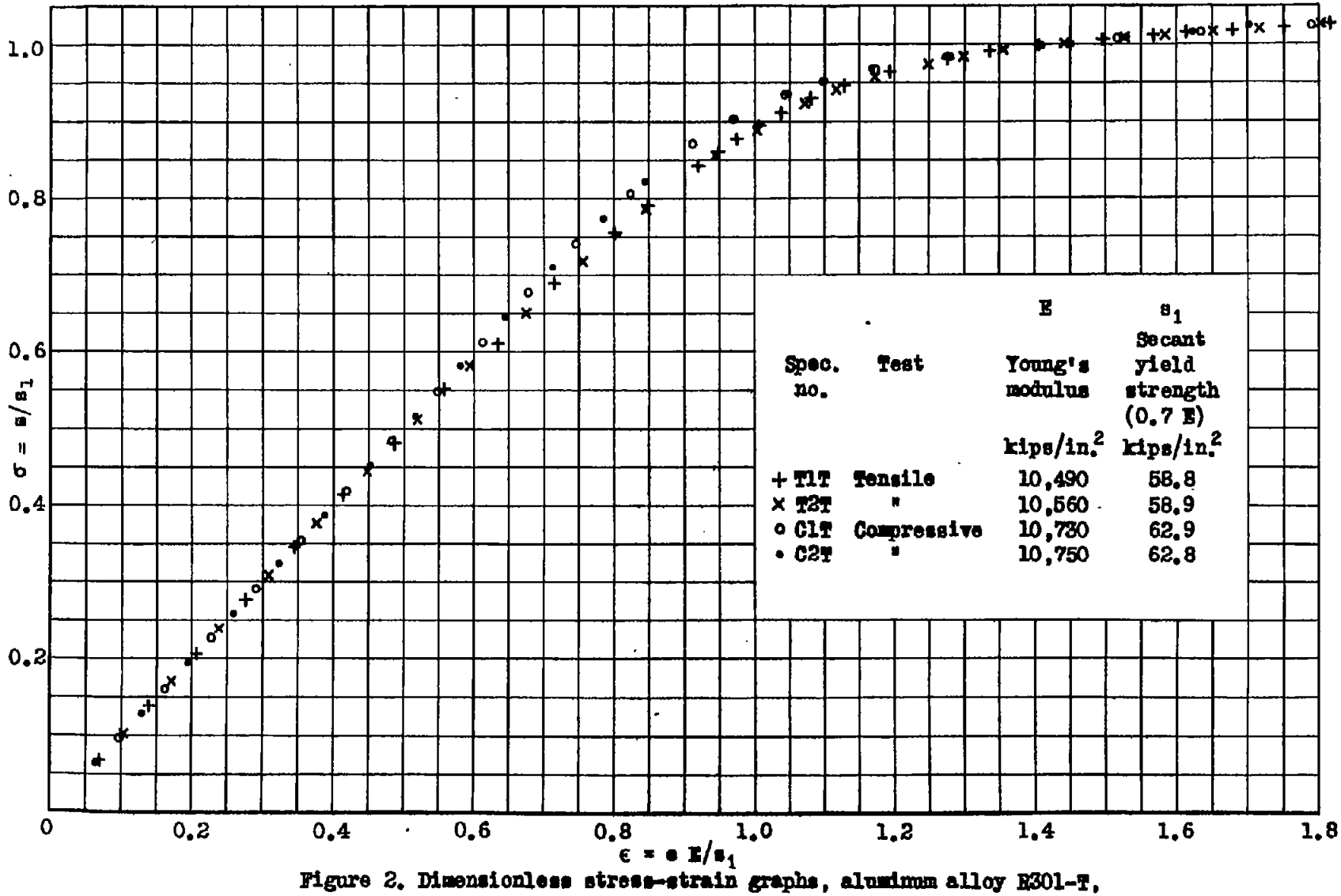

Figure 2. Dimensionless stress-strain graphs, aluminum alloy R301-T, transverse specimens 0.020 in. thick.

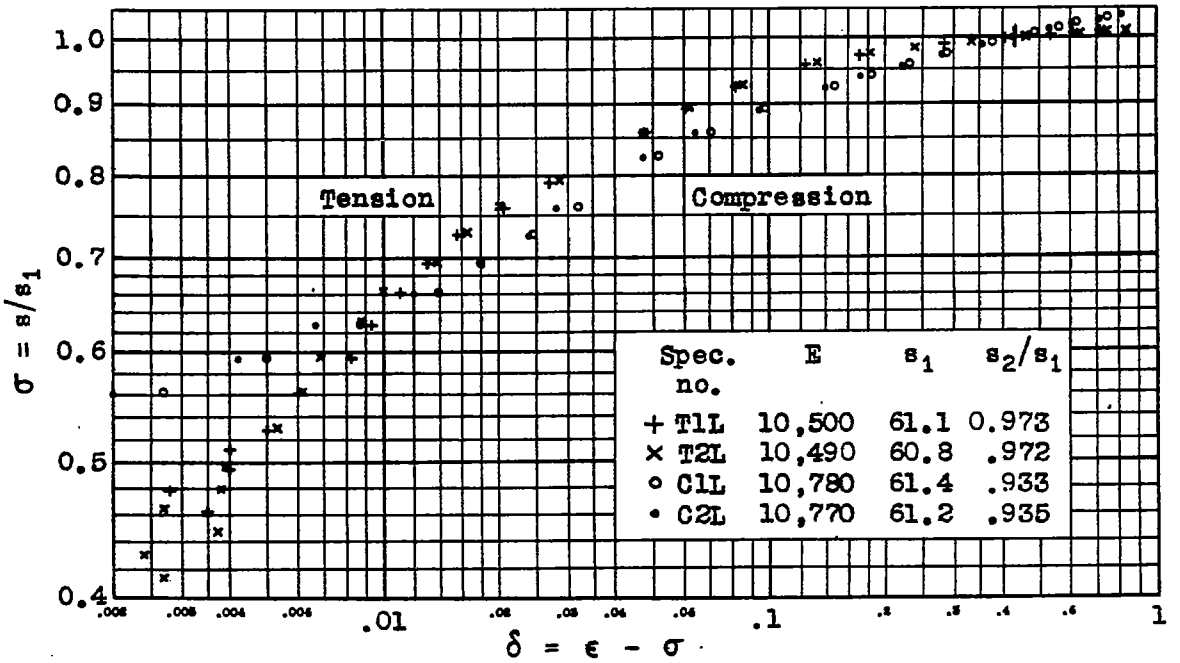

Figure 3. Dimensionless stress-deviation graphs, aluminum alloy R301-T, longitudinal specimens 0.020 in. thick.
E is Young's modulus, kips/in.^{2}
s_1 is secant yield strength (0.7 E), kips/in.^{2}
s_2 is secant yield strength (0.85 E), kips/in.^{2}

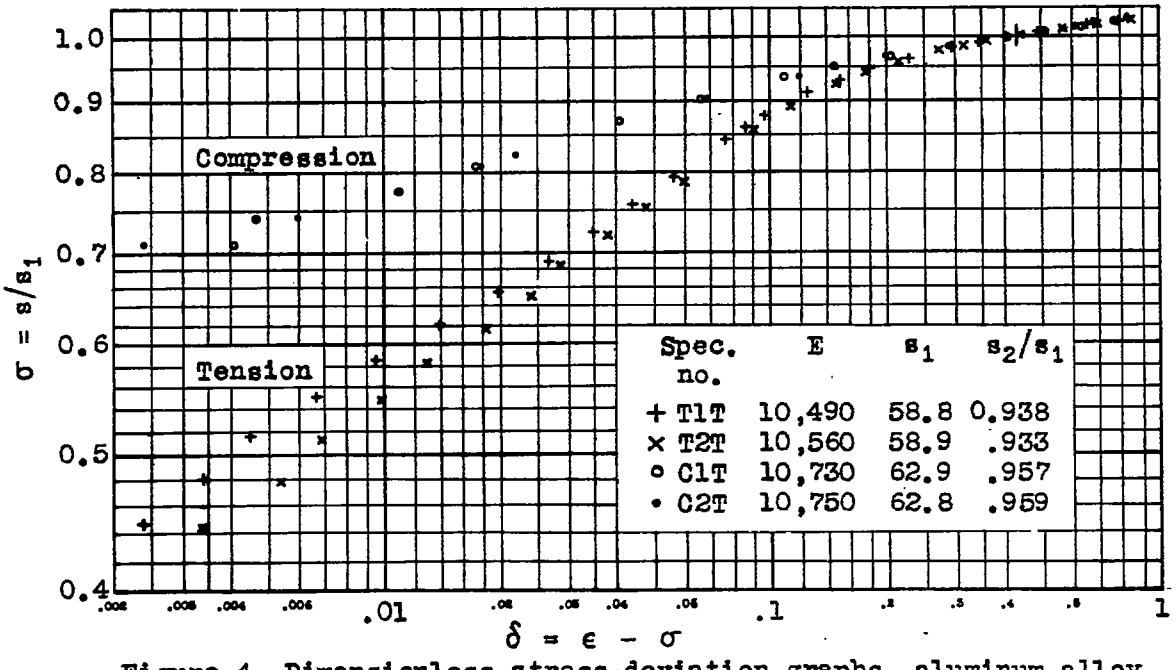

Figure 4. Dimensionless stress-deviation graphs, aluminum alloy R301-T, transverse specimens 0.020 in. thick.
E is Young's modulus, kips/in.^{2}
s_1 is secant yield strength (0.7 E), kips/in.^{2}
s_2 is secant yield strength (0.85 E), kips/in.^{2}

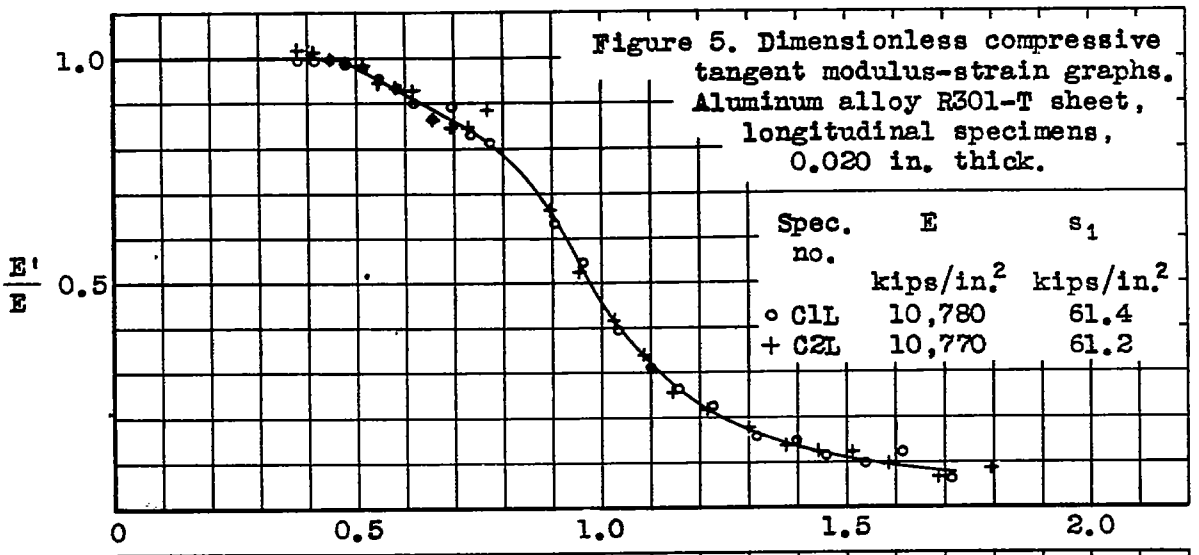

Figure 5. Dimensionless compressive tangent modulus-strain graphs. Aluminum alloy R301-T sheet, longitudinal specimens, 0.020 in. thick.

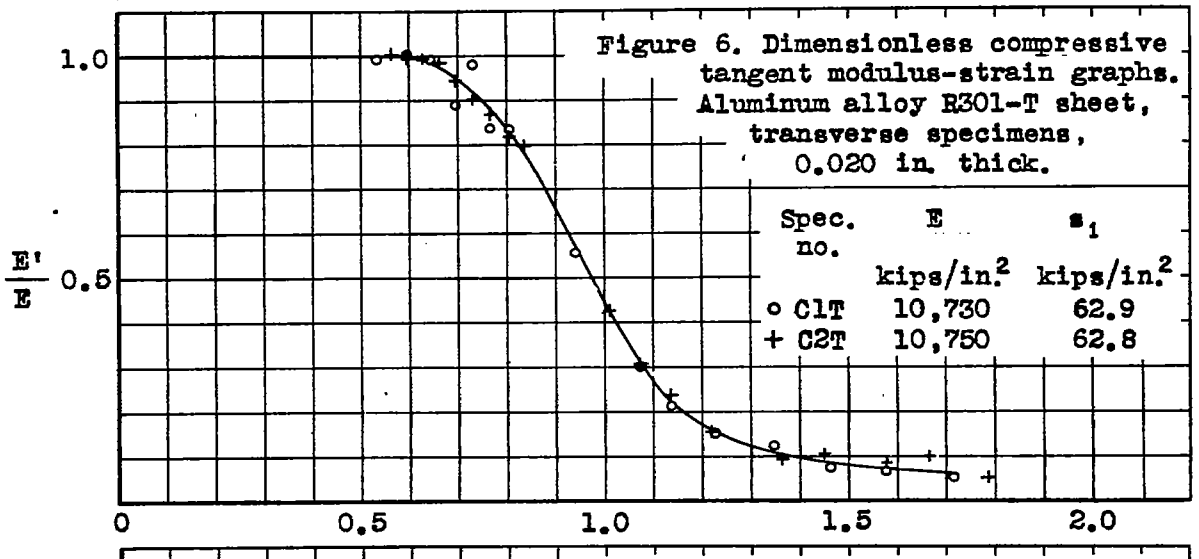

Figure 6. Dimensionless compressive tangent modulus-strain graphs. Aluminum alloy R301-T sheet, transverse specimens, 0.020 in. thick.

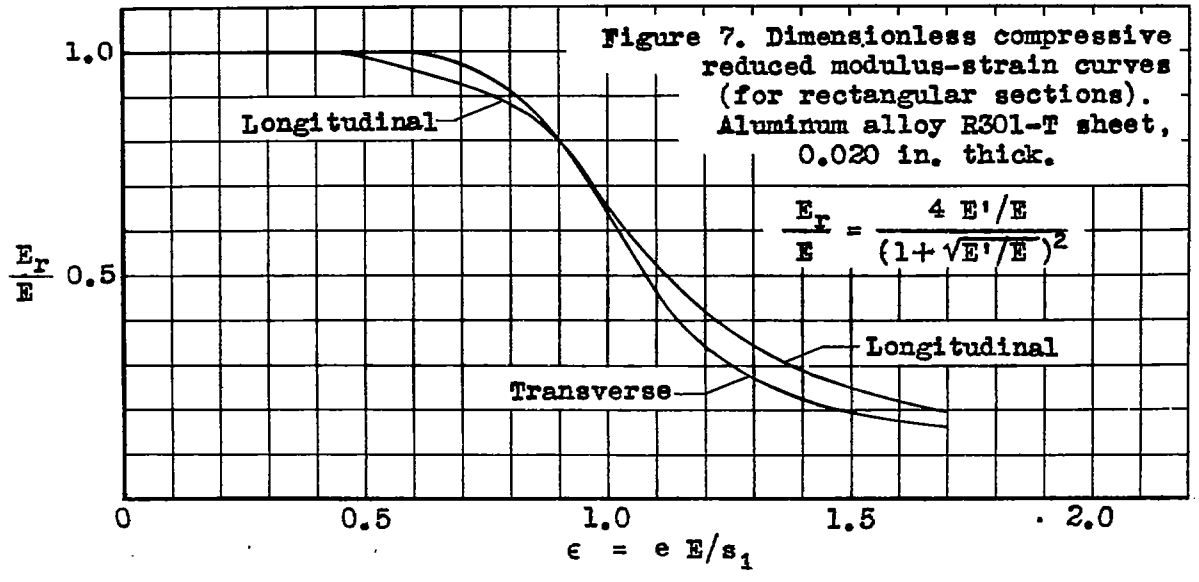

Figure 7. Dimensionless compressive reduced modulus-strain curves (for rectangular sections). Aluminum alloy R301-T sheet, 0.020 in. thick.

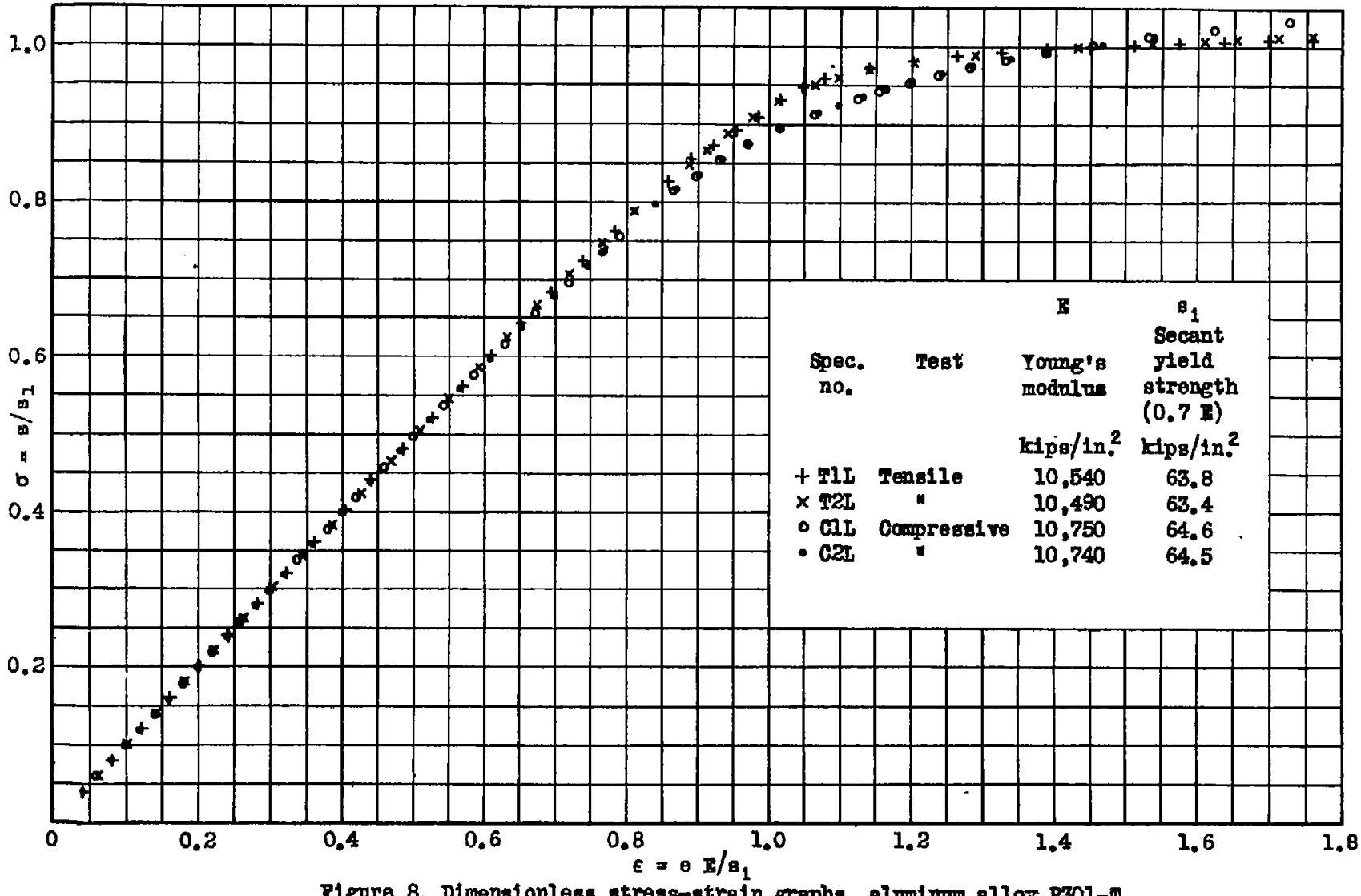

Figure 8. Dimensionless stress-strain graphs, aluminum alloy R301-T, longitudinal specimens 0.032 in. thick.

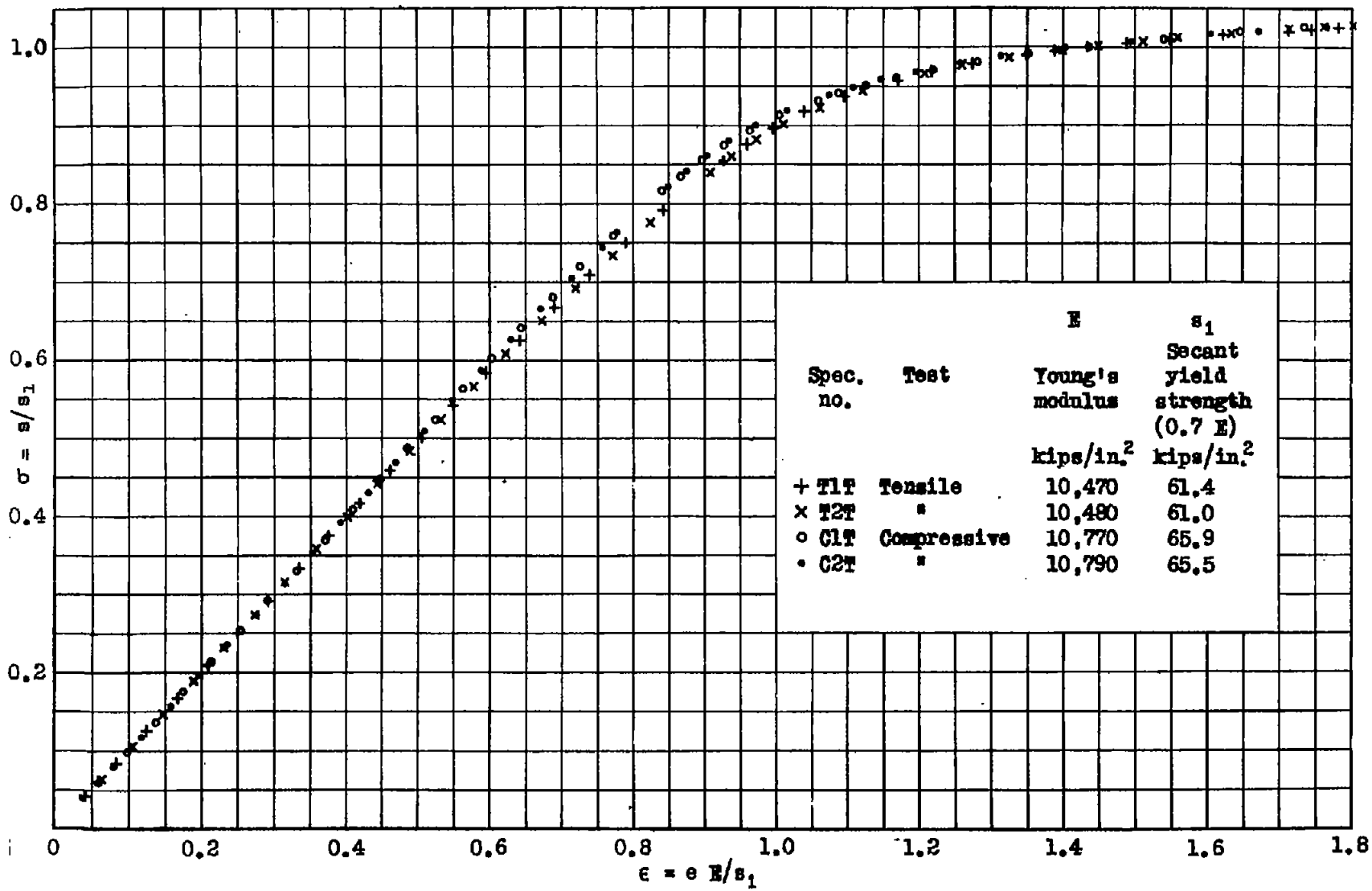

Figure 9. Dimensionless stress-strain graphs, aluminum alloy R301-T, transverse specimens 0.032 in. thick.

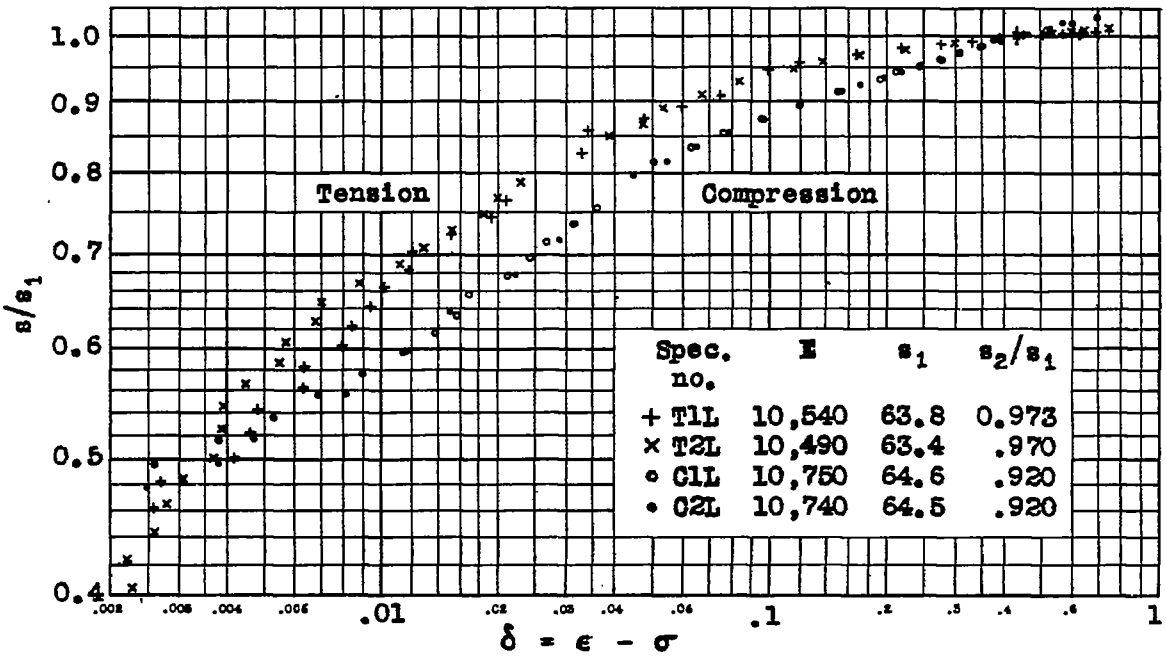

Figure 10. Dimensionless stress-deviation graphs, aluminum alloy R301-T, longitudinal specimens 0.032 in. thick.
E is Young's modulus, kips/in.^{2}
s_1 is secant yield strength (0.7 E), kips/in.^{2}
s_2 is secant yield strength (0.85 E), kips/in.^{2}

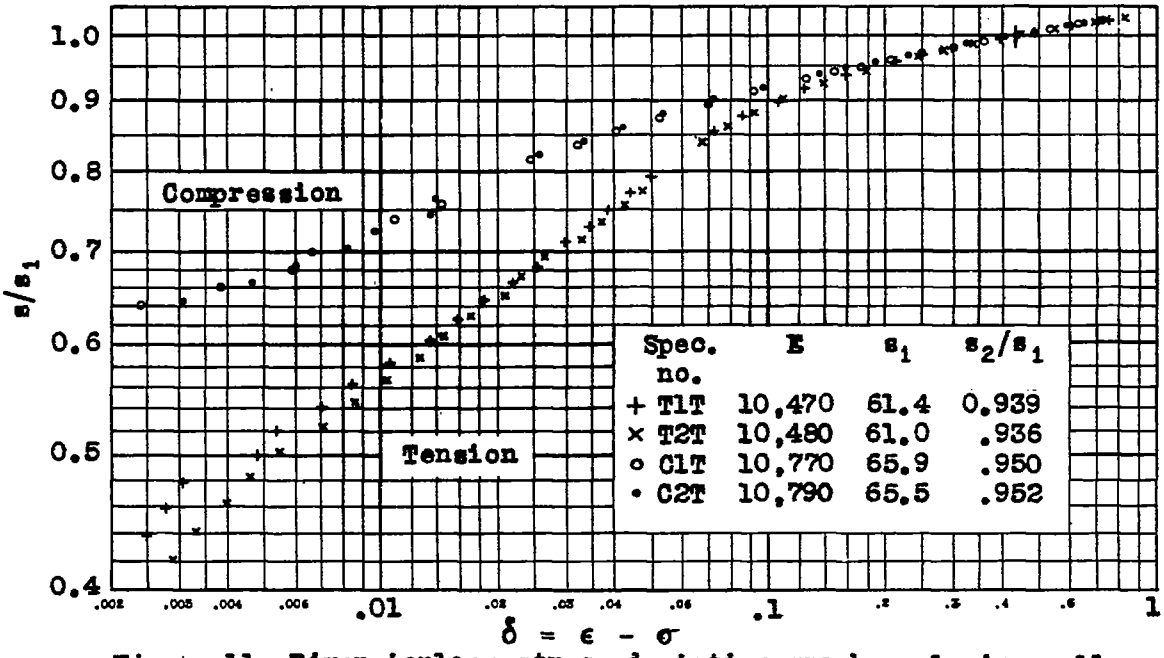

Figure 11. Dimensionless stress-deviation graphs, aluminum alloy R301-T, transverse specimens 0.032 in. thick.
E is Young's modulus, kips/in.^{2}
s_1 is secant yield strength (0.7 E), kips/in.^{2}
s_2 is secant yield strength (0.85 E), kips/in.^{2}

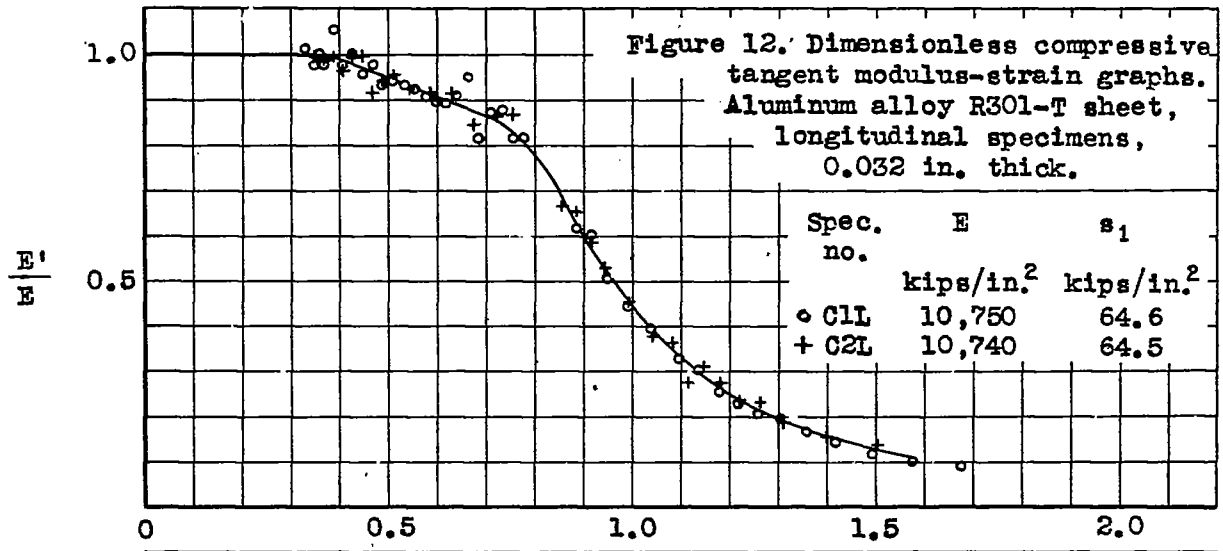

Figure 12. Dimensionless compressive tangent modulus-strain graphs. Aluminum alloy R301-T sheet, longitudinal specimens, 0.032 in. thick.

Spec. no.	E kips/in.^{2}	s_1 kips/in.^{2}
○ C1L	10,750	64.6
+ C2L	10,740	64.5

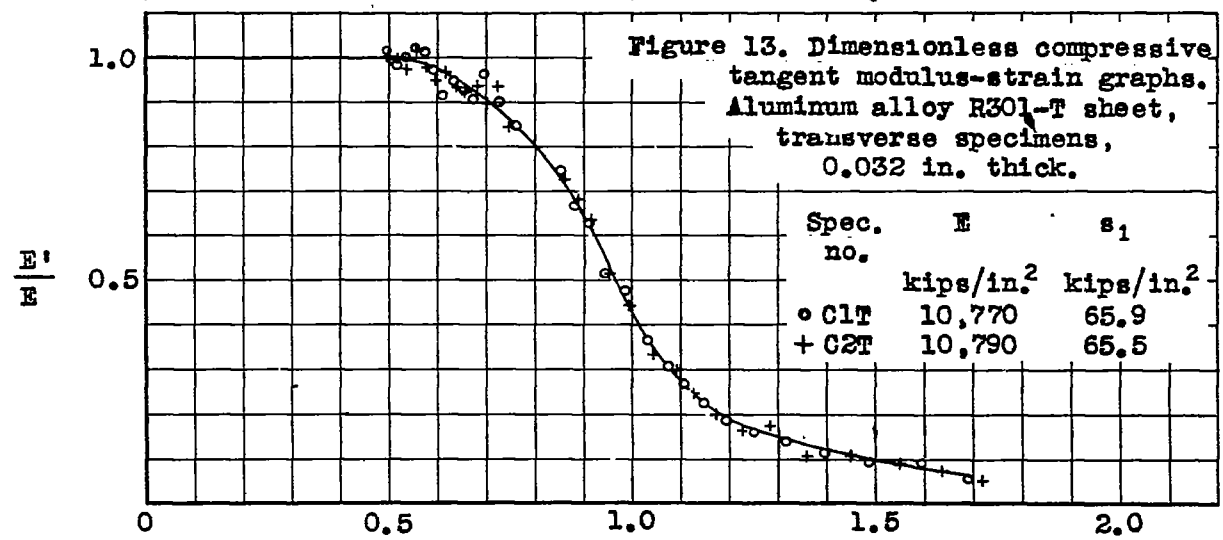

Figure 13. Dimensionless compressive tangent modulus-strain graphs. Aluminum alloy R301-T sheet, transverse specimens, 0.032 in. thick.

Spec. no.	E kips/in.^{2}	s_1 kips/in.^{2}
○ C1T	10,770	65.9
+ C2T	10,790	65.5

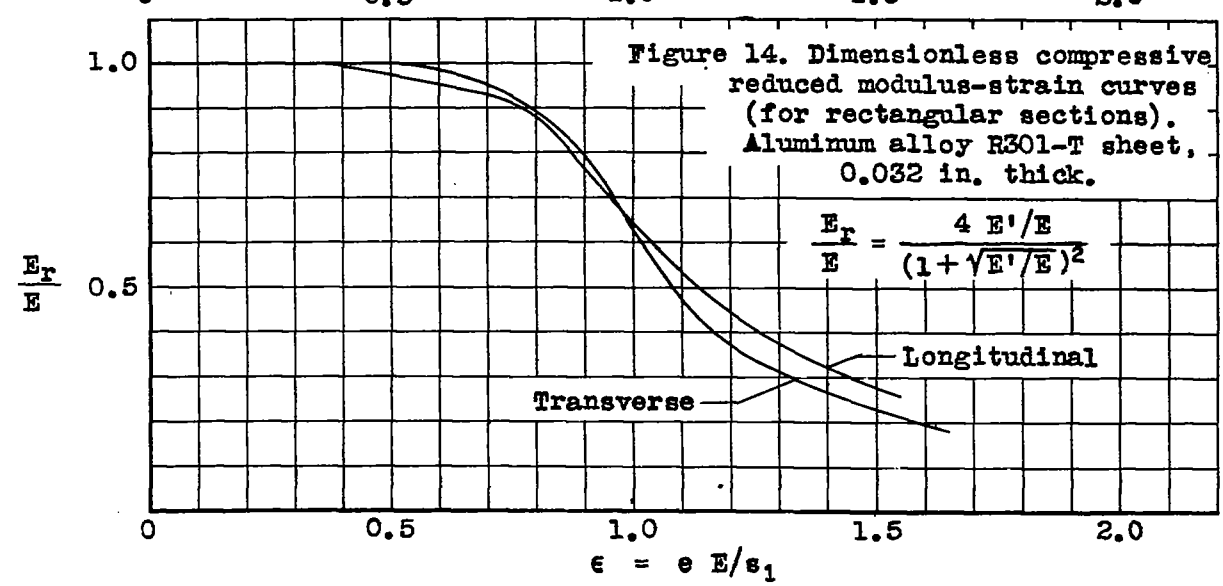

Figure 14. Dimensionless compressive reduced modulus-strain curves (for rectangular sections). Aluminum alloy R301-T sheet, 0.032 in. thick.

$$\frac{E_r}{E} = \frac{4\,E'/E}{(1+\sqrt{E'/E})^2}$$

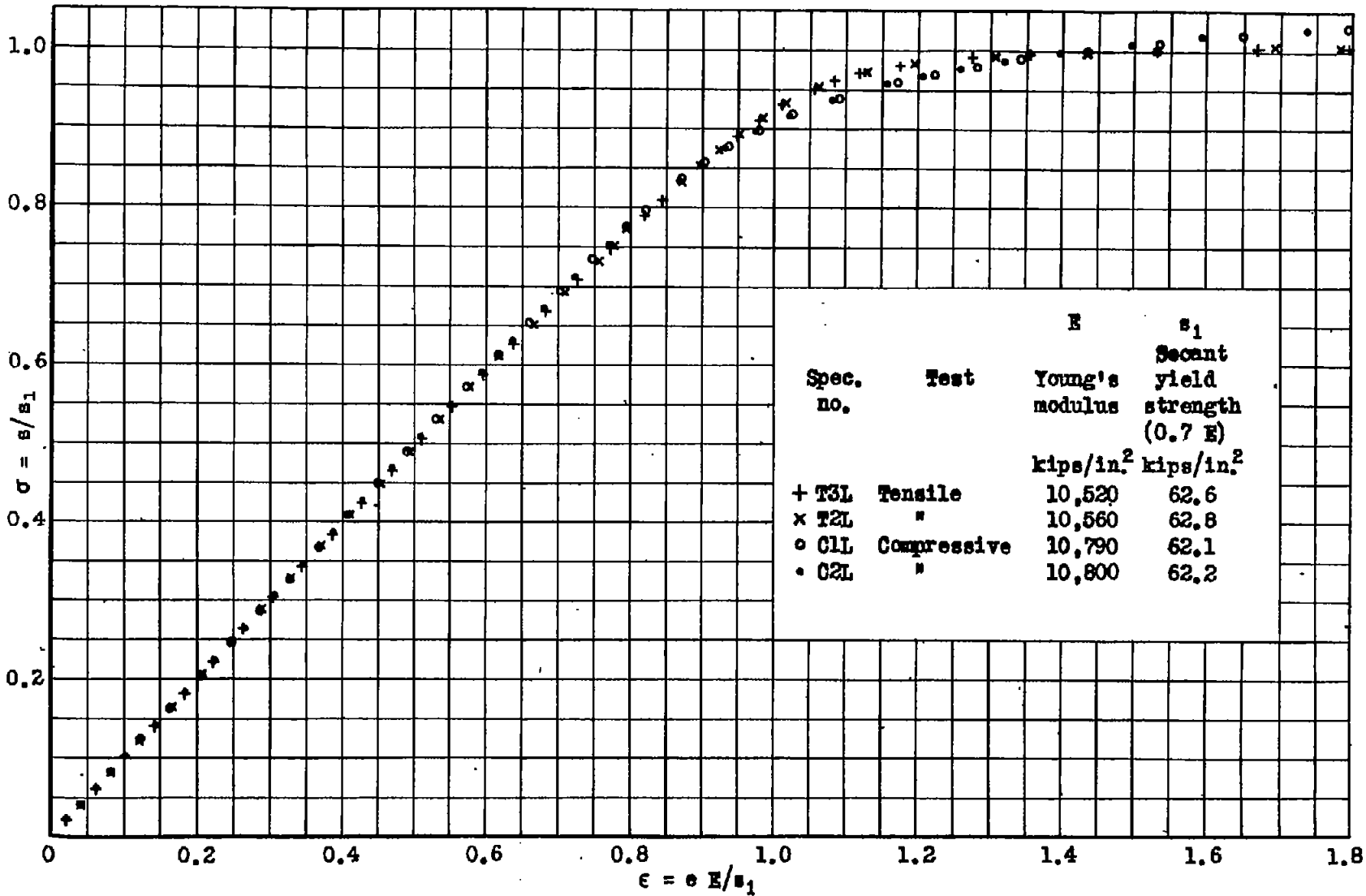

Figure 15. Dimensionless stress-strain graphs, aluminum alloy R301-T, longitudinal specimens 0.064 in. thick.

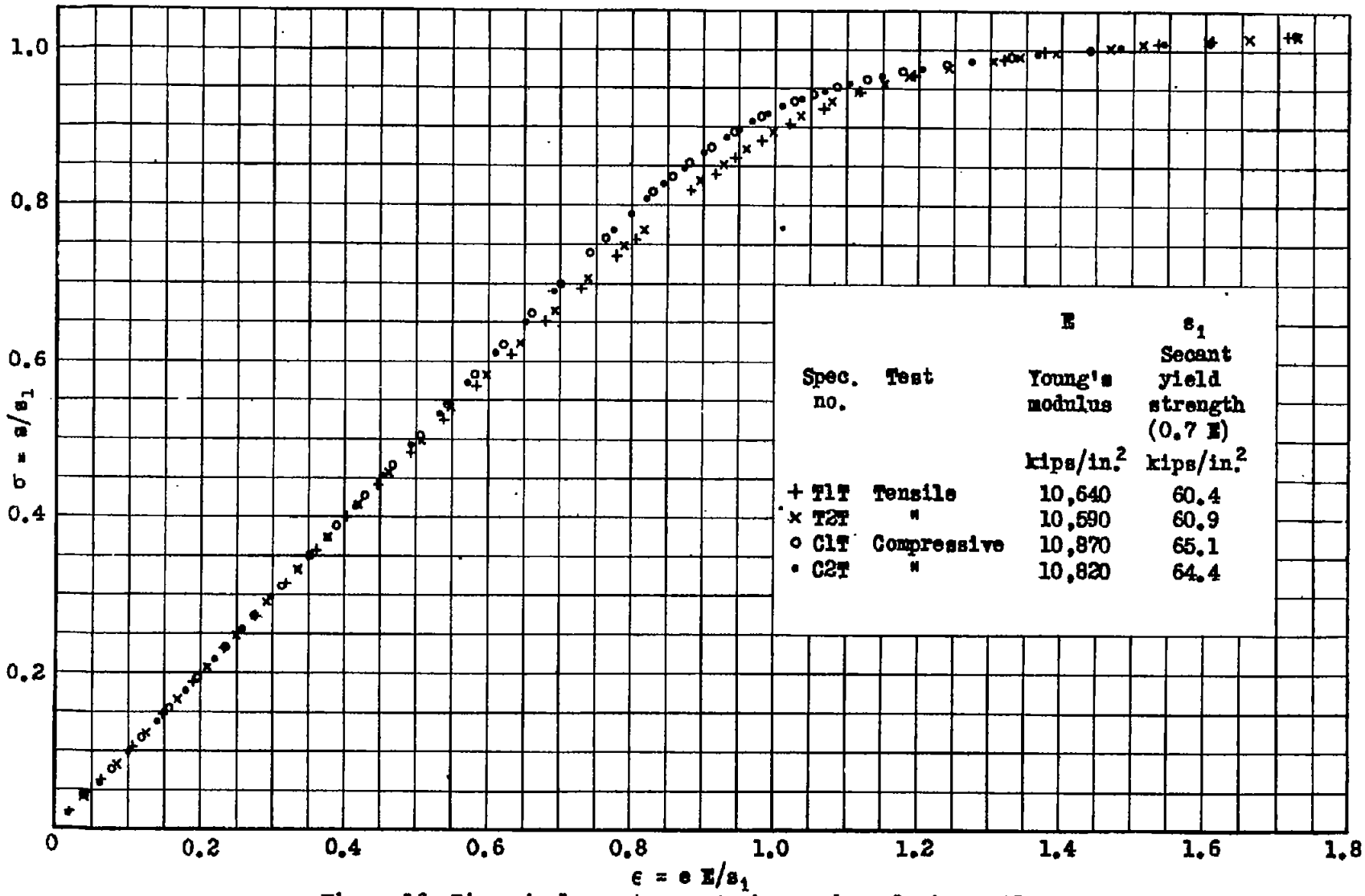

Figure 16. Dimensionless stress-strain graphs, aluminum alloy RZ01-T, transverse specimens 0.064 in. thick.

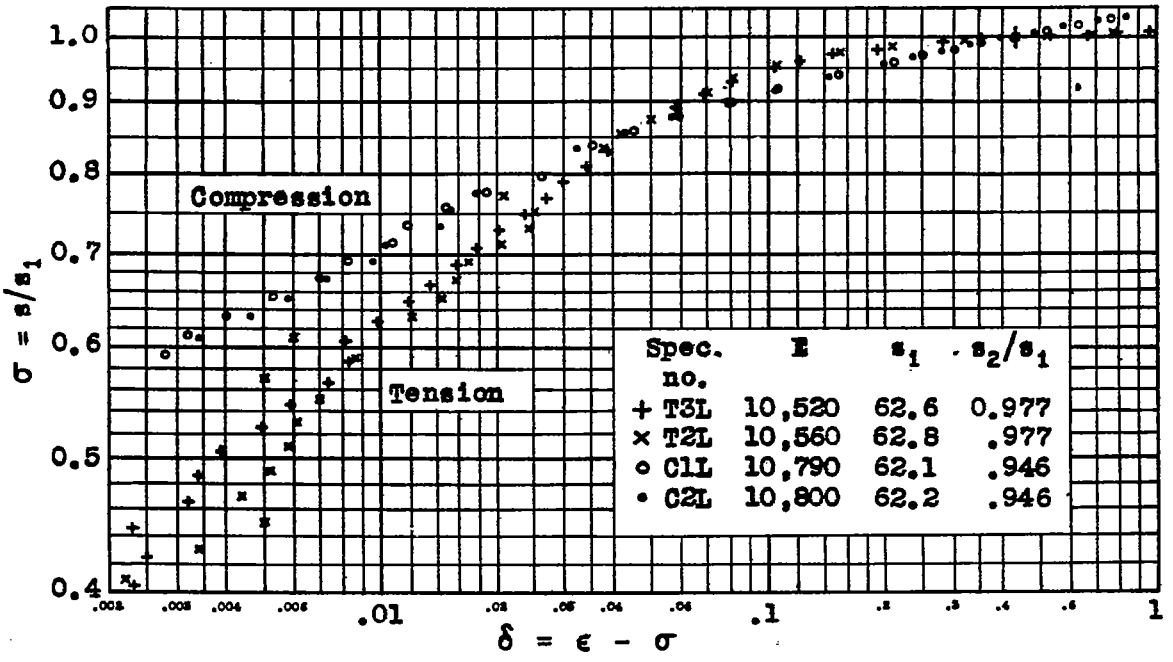

Figure 17. Dimensionless stress-deviation graphs, aluminum alloy R301-T, longitudinal specimens 0.064 in. thick.
E is Young's modulus, kips/in.^{2}
s_1 is secant yield strength (0.7 E), kips/in.^{2}
s_2 is secant yield strength (0.85 E), kips/in.^{2}

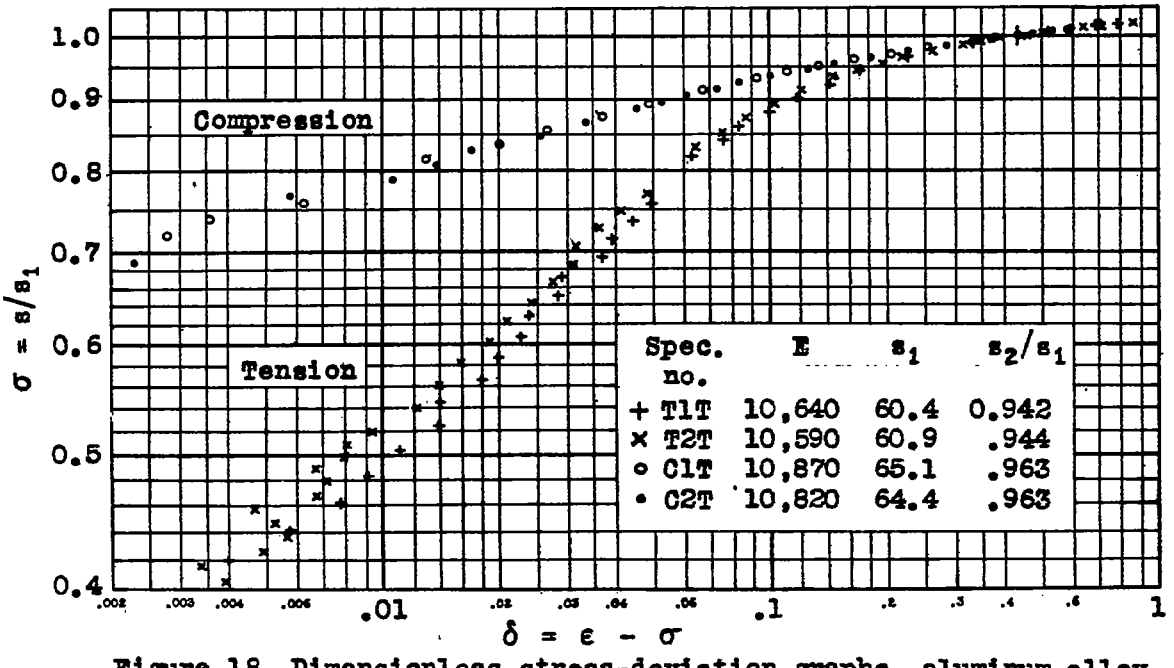

Figure 18. Dimensionless stress-deviation graphs, aluminum alloy R301-T, transverse specimens 0.064 in. thick.
E is Young's modulus, kips/in.^{2}
s_1 is secant yield strength (0.7 E), kips/in.^{2}
s_2 is secant yield strength (0.85 E), kips/in.^{2}

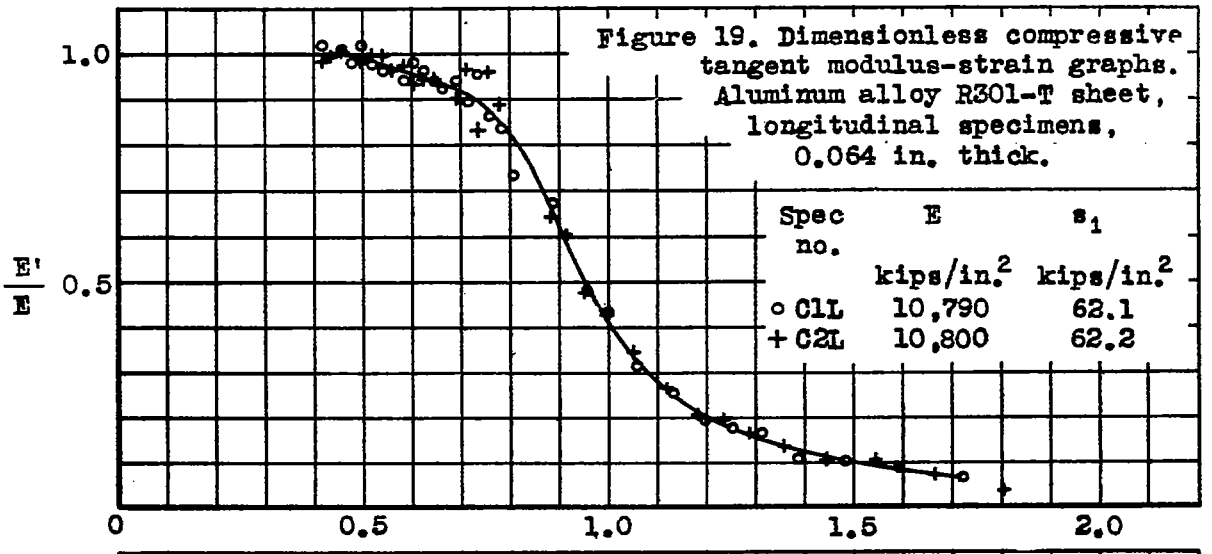

Figure 19. Dimensionless compressive tangent modulus-strain graphs. Aluminum alloy R301-T sheet, longitudinal specimens, 0.064 in. thick.

Spec no.	E kips/in.^{2}	s_1 kips/in.^{2}
○ C1L	10,790	62.1
+ C2L	10,800	62.2

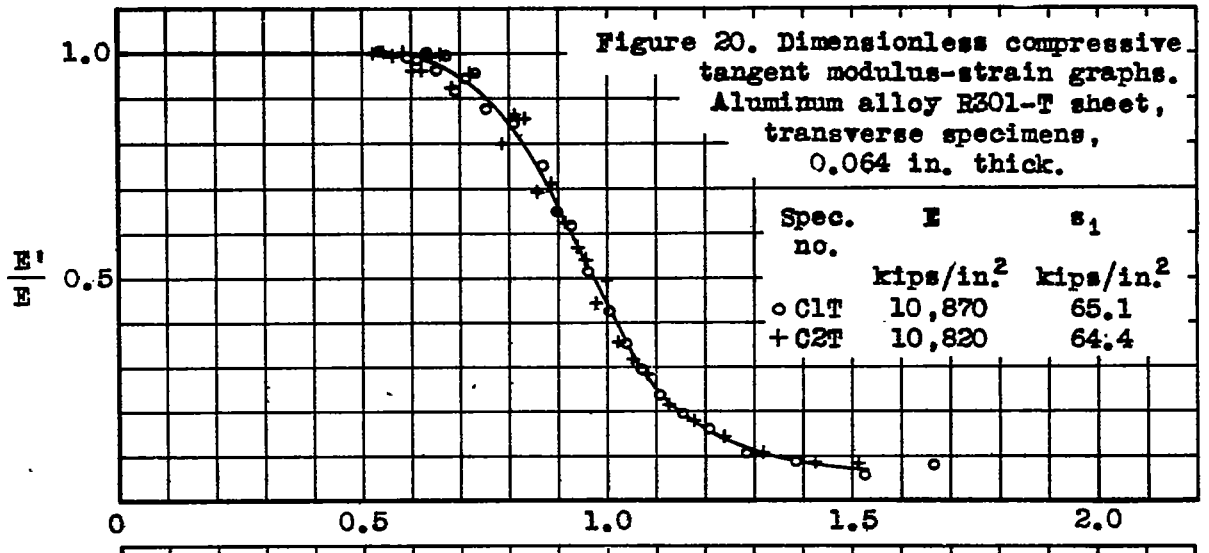

Figure 20. Dimensionless compressive tangent modulus-strain graphs. Aluminum alloy R301-T sheet, transverse specimens, 0.064 in. thick.

Spec. no.	E kips/in.^{2}	s_1 kips/in.^{2}
○ C1T	10,870	65.1
+ C2T	10,820	64.4

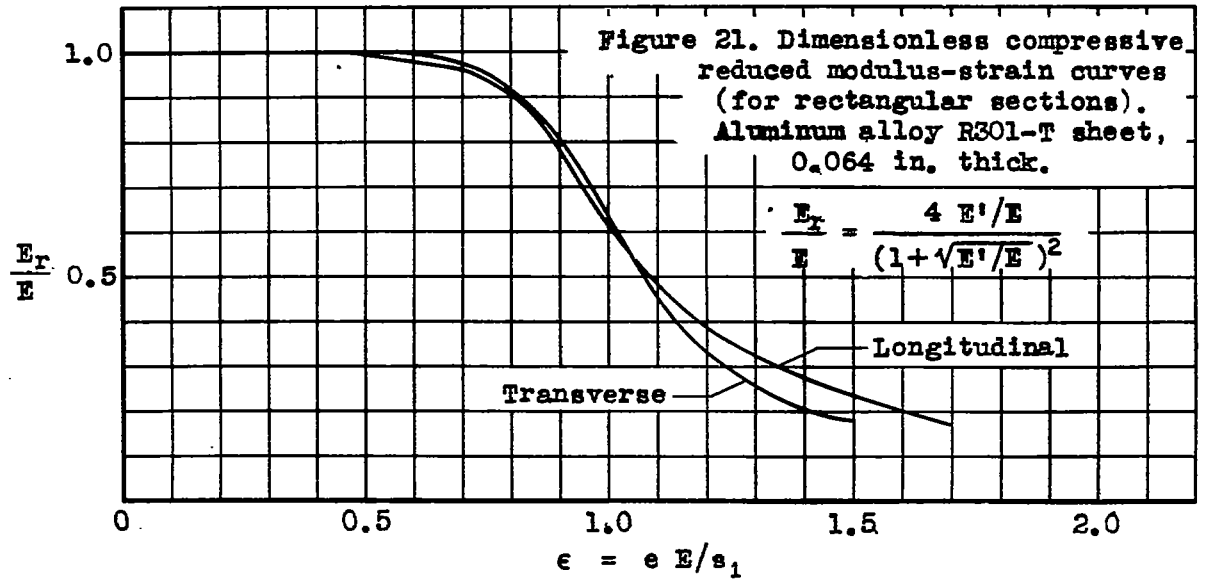

Figure 21. Dimensionless compressive reduced modulus-strain curves (for rectangular sections). Aluminum alloy R301-T sheet, 0.064 in. thick.

$$\frac{E_r}{E} = \frac{4\,E'/E}{(1+\sqrt{E'/E})^2}$$

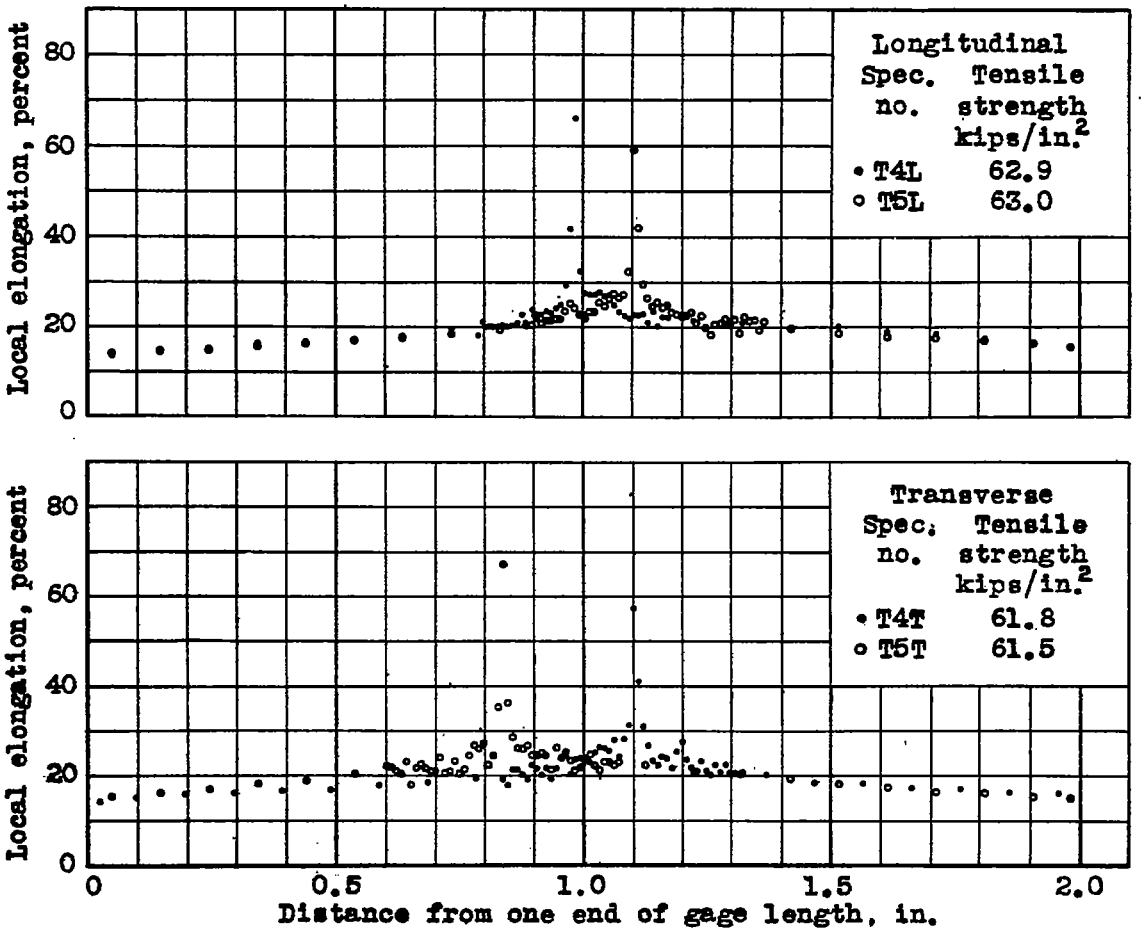

Figure 22. Local elongation, aluminum alloy R301-W sheet, 0.020 in. thick.

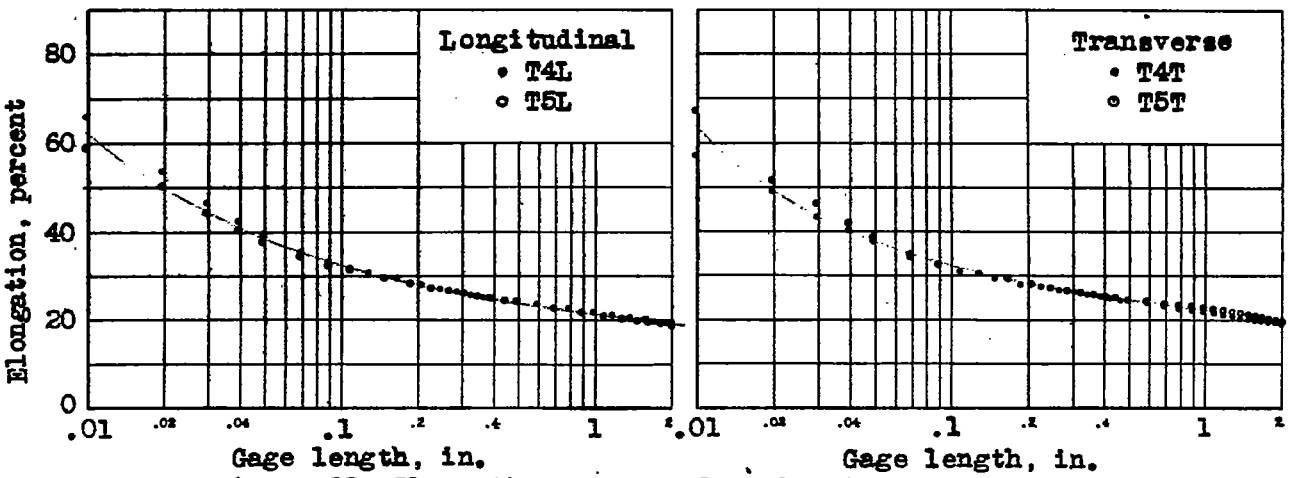

Figure 23. Elongation vs gage length, aluminum alloy R301-W sheet, 0.020 in. thick.

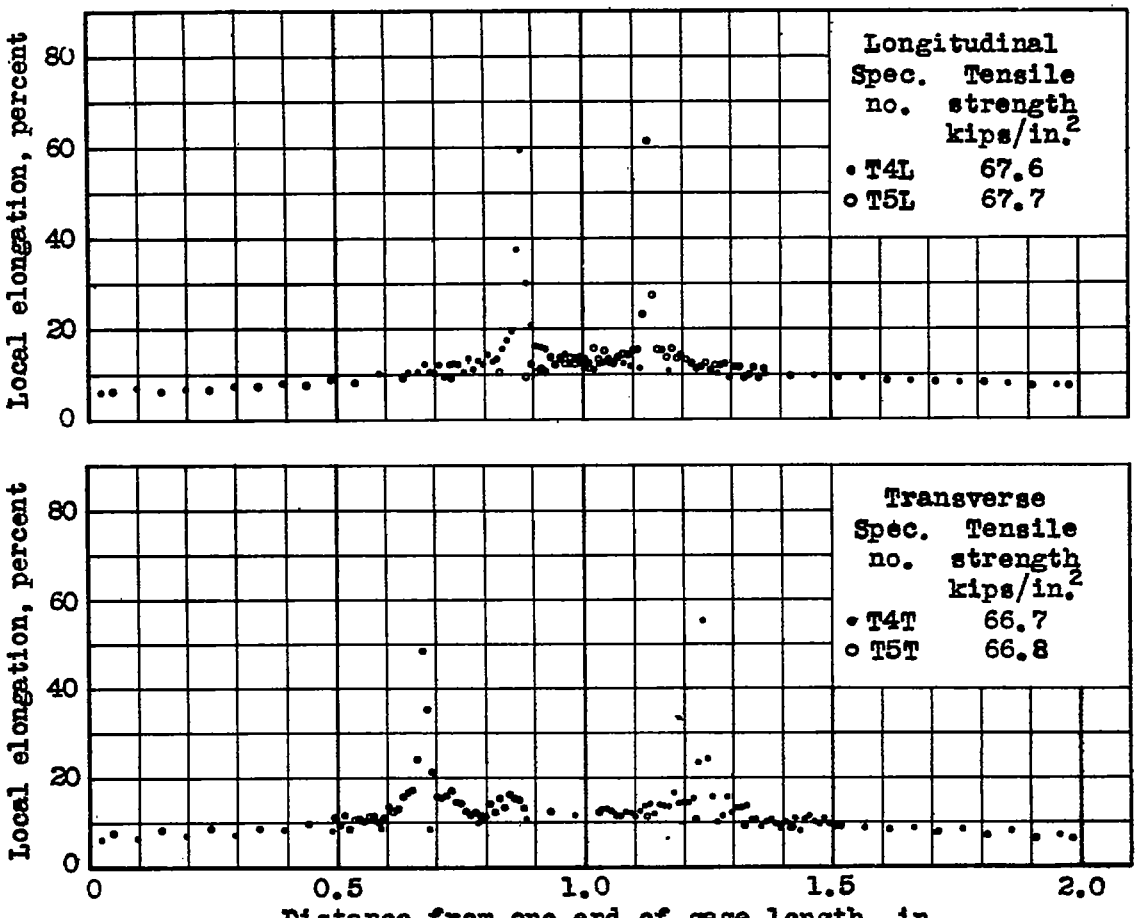

Figure 24. Local elongation, aluminum alloy R301-T sheet, 0.020 in. thick.

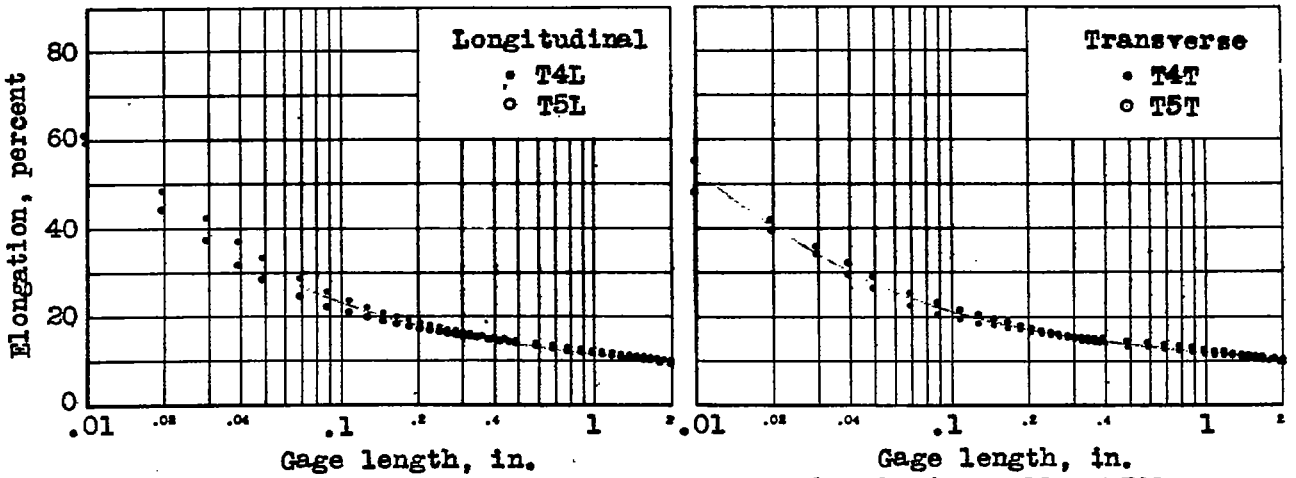

Figure 25. Elongation vs gage length, aluminum alloy R301-T sheet, 0.020 in. thick.

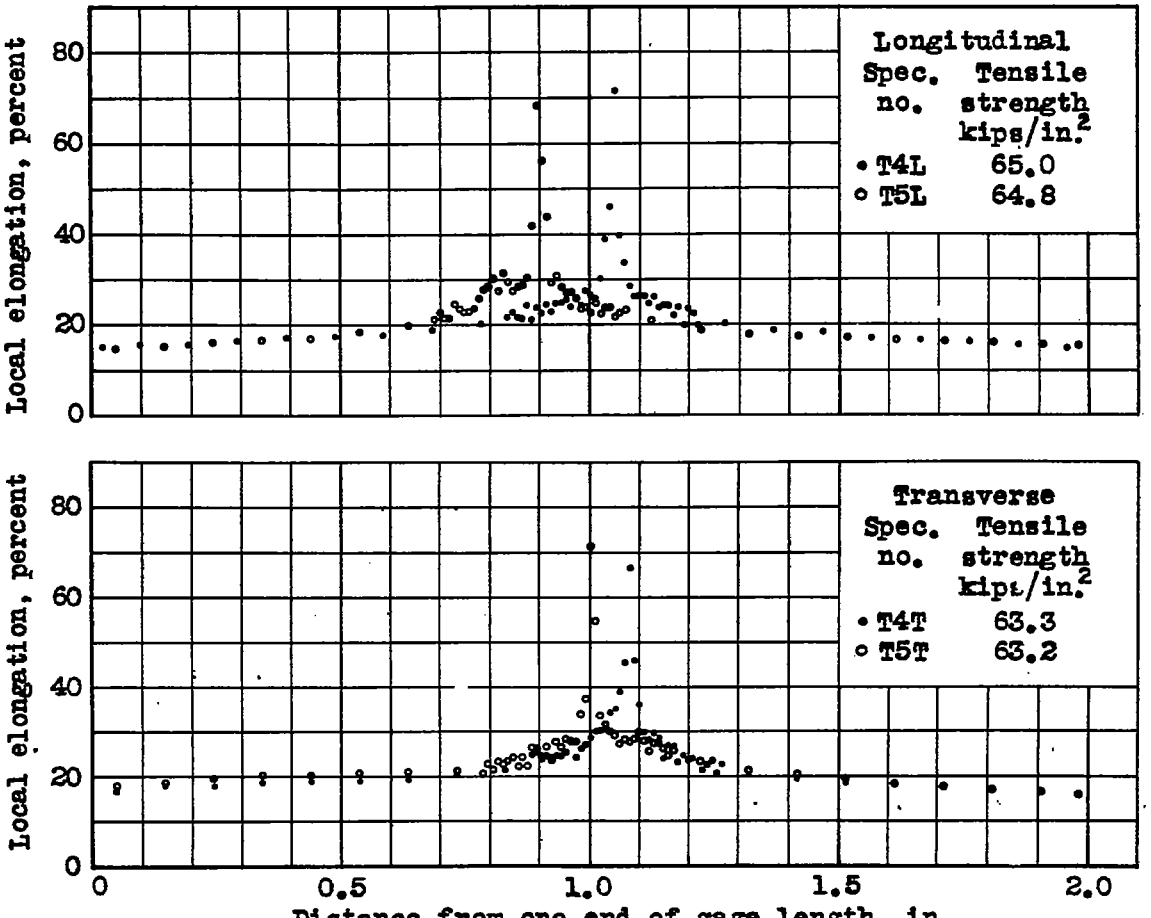

Figure 26. Local elongation, aluminum alloy R301-W sheet, 0.032 in. thick.

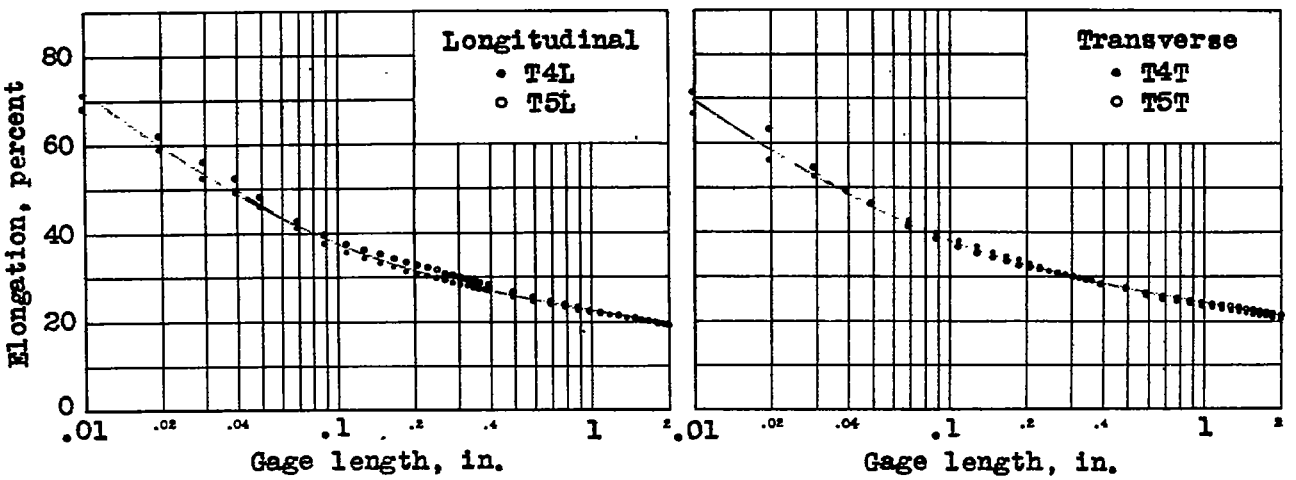

Figure 27. Elongation vs gage length, aluminum alloy R301-W sheet, 0.032 in. thick.

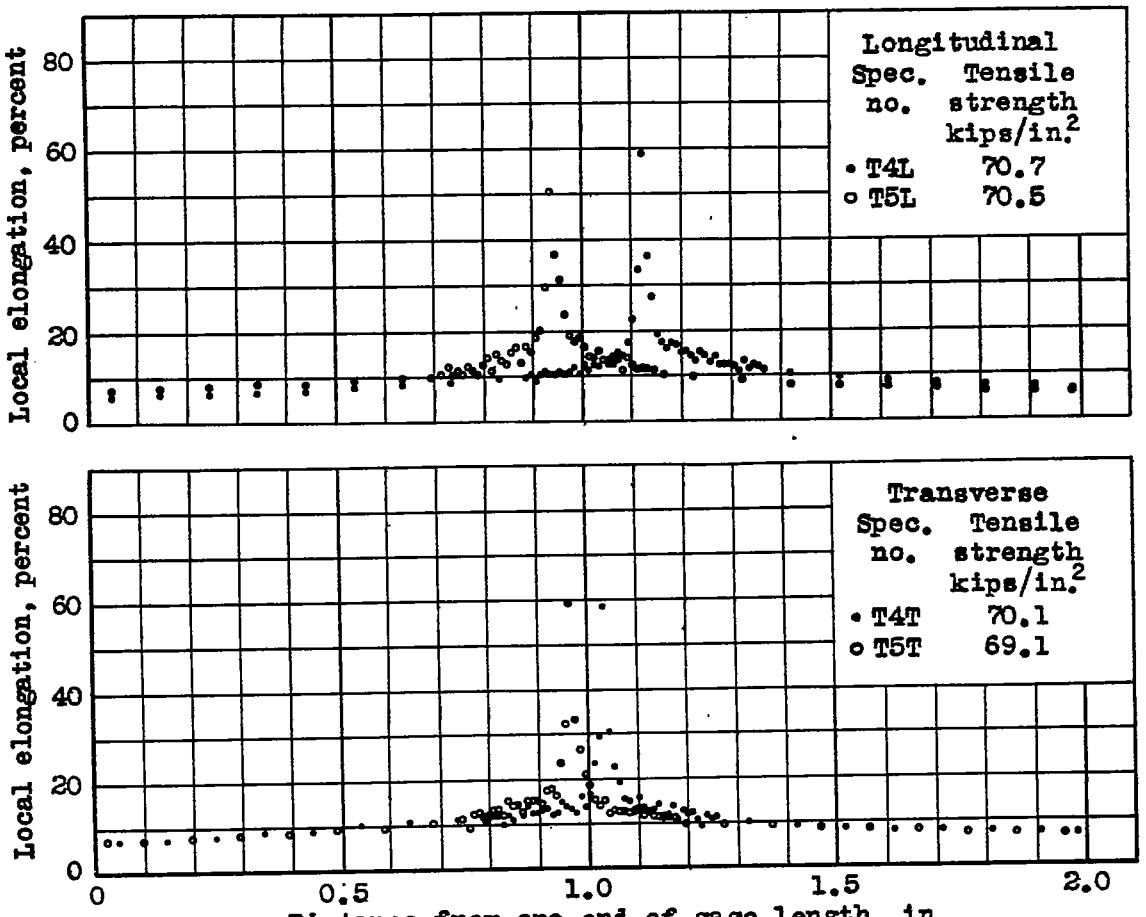

Figure 28. Local elongation, aluminum alloy R301-T sheet, 0.032 in. thick.

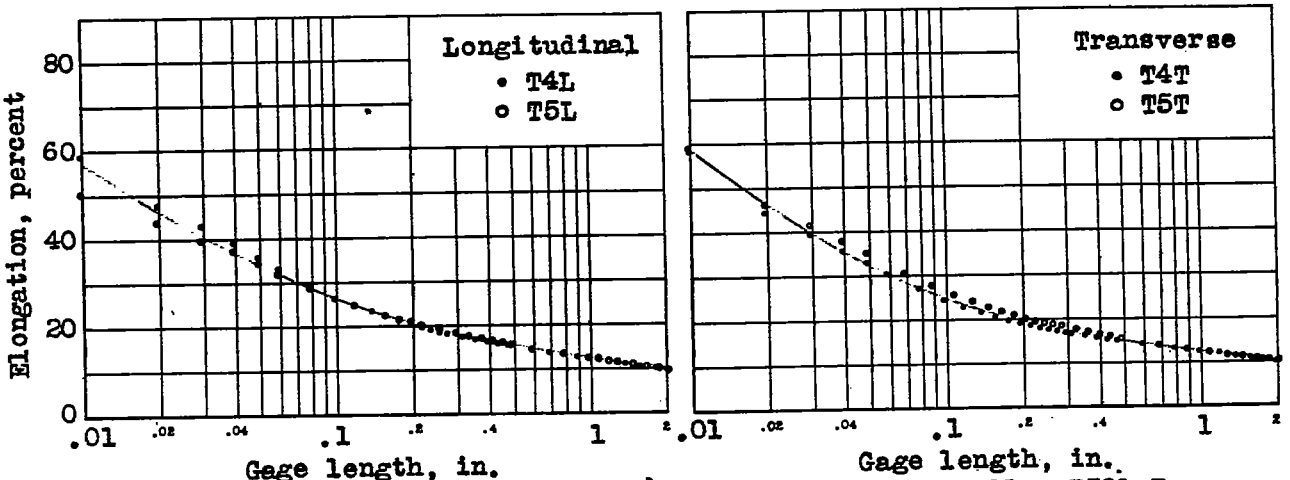

Figure 29. Elongation vs gage length, aluminum alloy R301-T sheet, 0.032 in. thick.

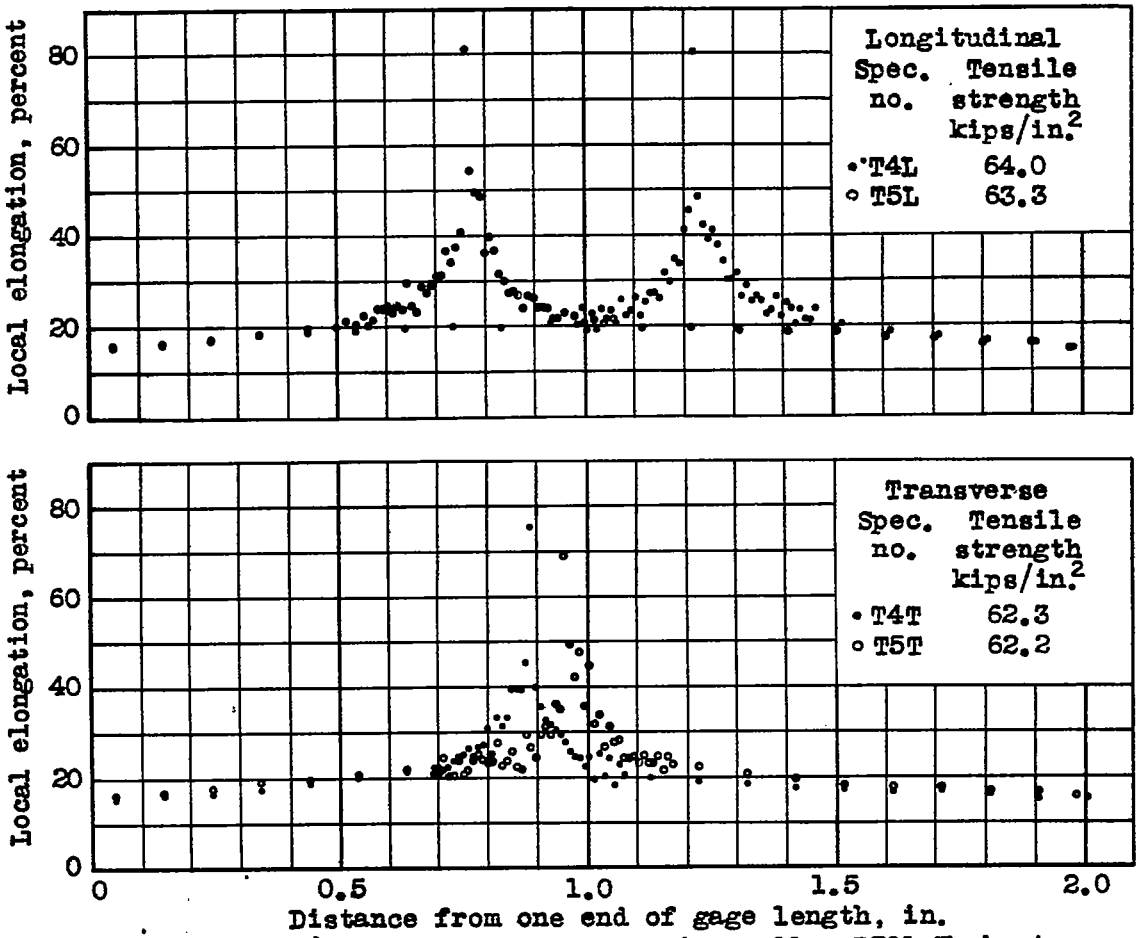

Figure 30. Local elongation, aluminum alloy R301-W sheet, 0.064 in. thick.

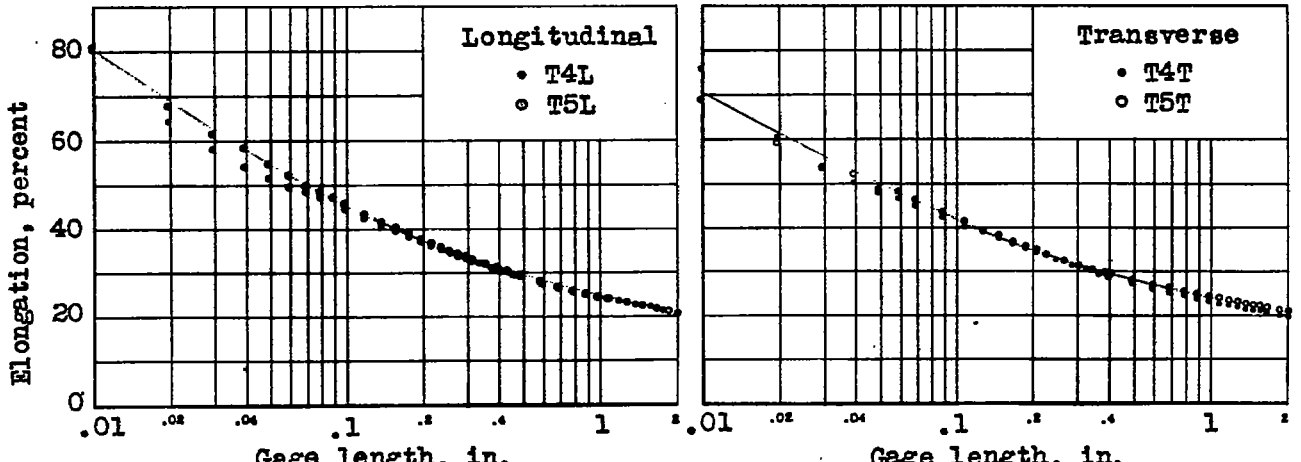

Figure 31. Elongation vs gage length, aluminum alloy R301-W sheet, 0.064 in. thick.

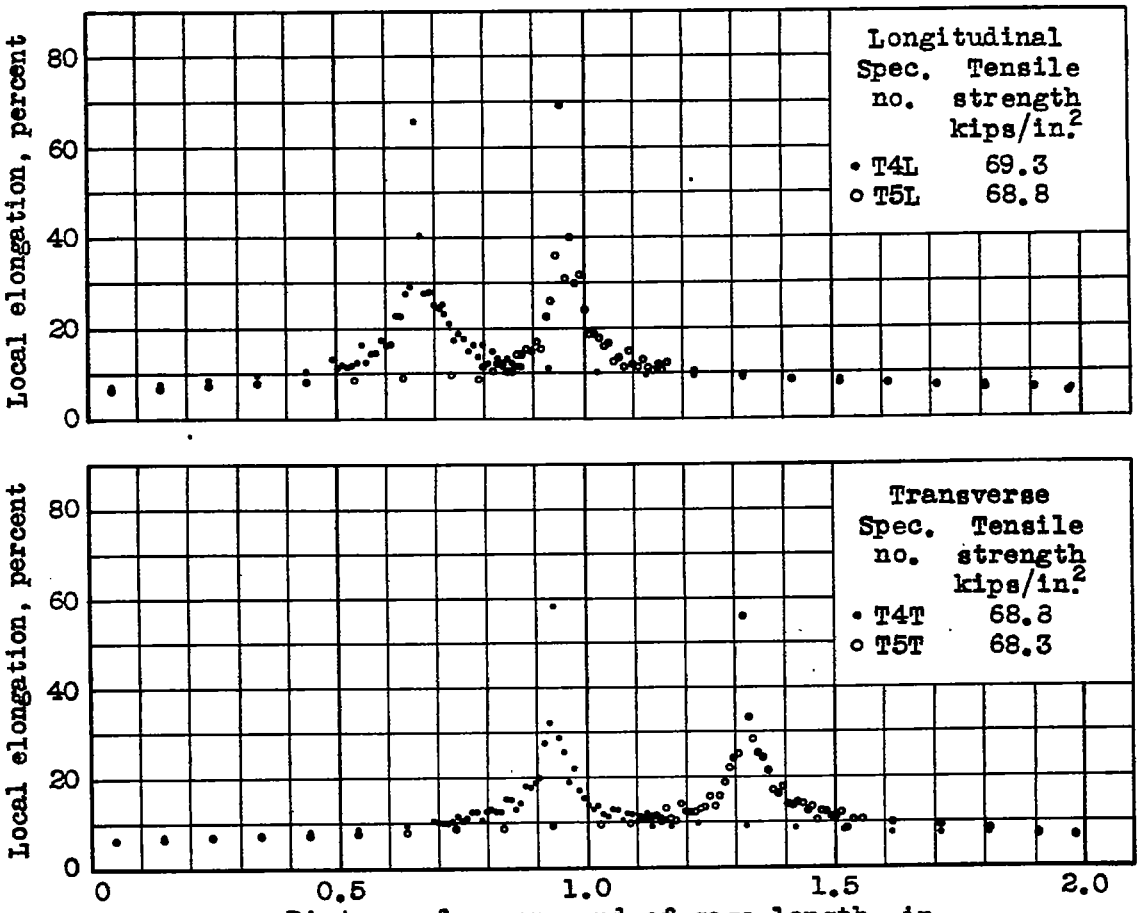

Figure 32. Local elongation, aluminum alloy R301-T sheet, 0.064 in. thick.

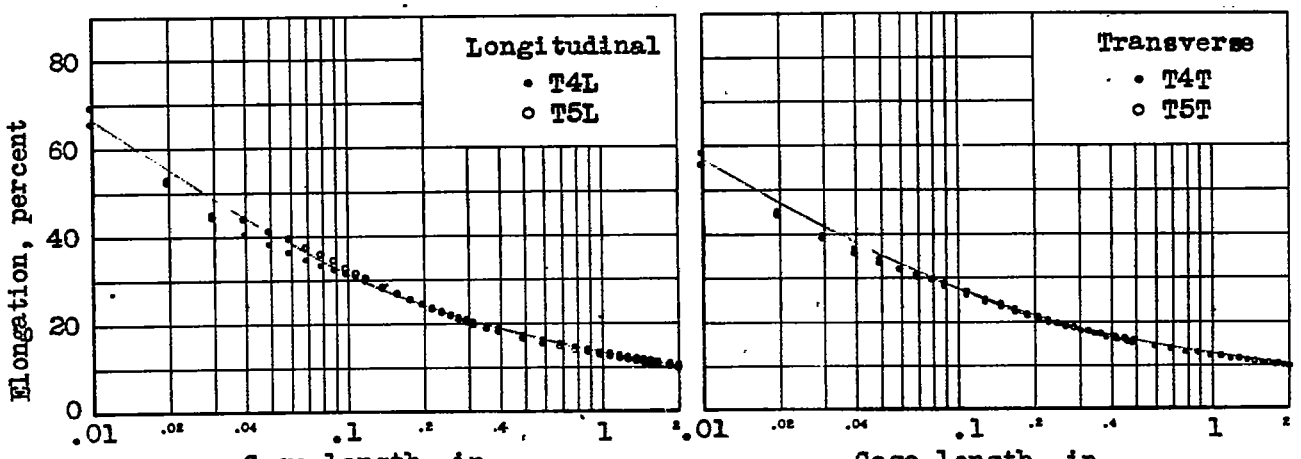

Figure 33. Elongation vs gage length, aluminum alloy R301-T sheet, 0.064 in. thick.

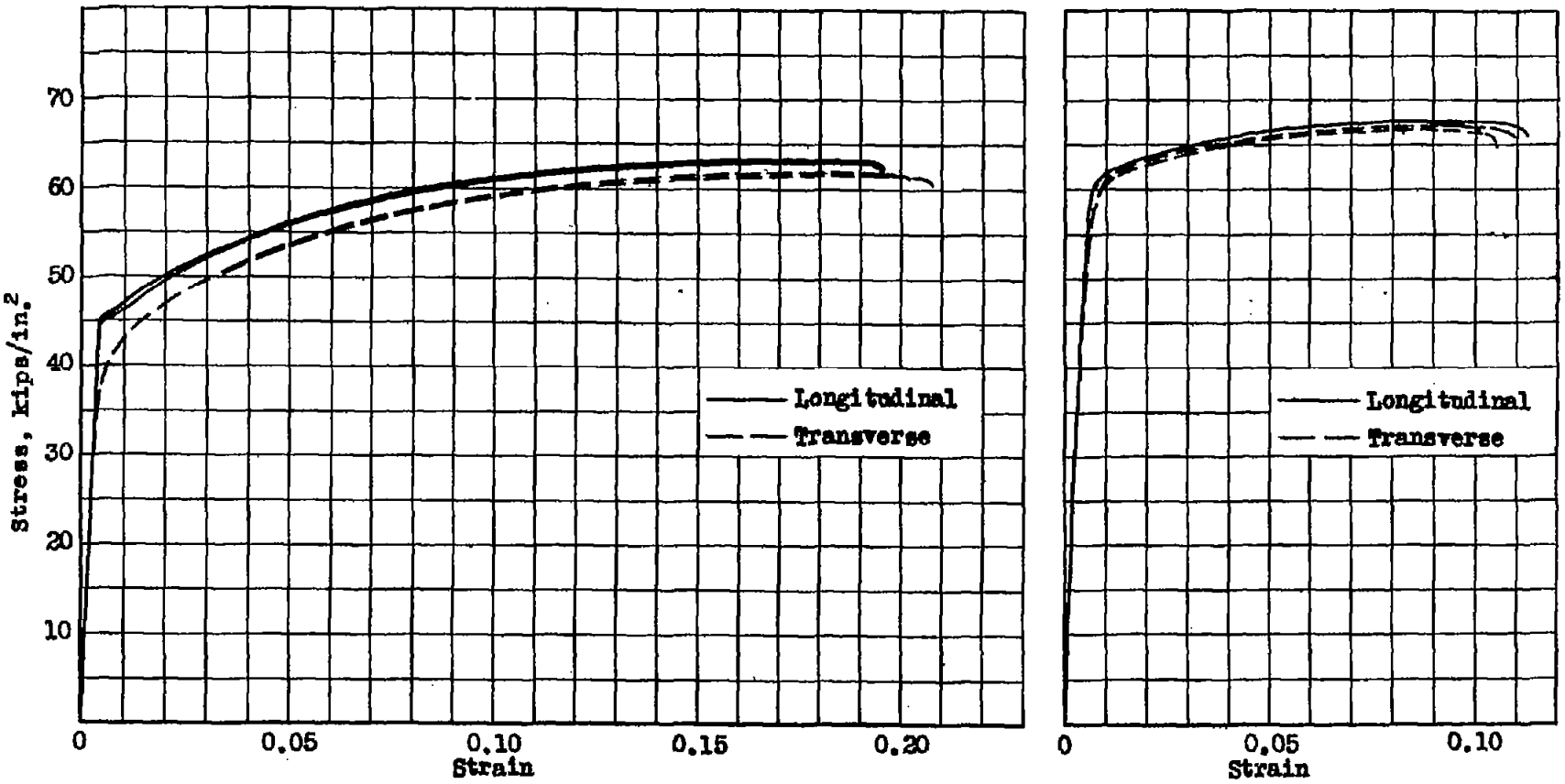

Aluminum alloy R301-W

Spec. no.	Tensile strength kips/in.²	Elongation in 2 in. percent
T7L	63.2	18.8
T8L	63.0	18.8
T7T	61.8	19.7
T8T	61.6	20.0

Aluminum alloy R301-T

Spec. no.	Tensile strength kips/in.²	Elongation in 2 in. percent
T7L	67.7	10.8
T8L	67.7	9.8
T7T	67.1	10.1
T8T	66.7	10.0

Figure 34. Tensile stress-strain curves to failure, thickness of sheet 0.020 in.

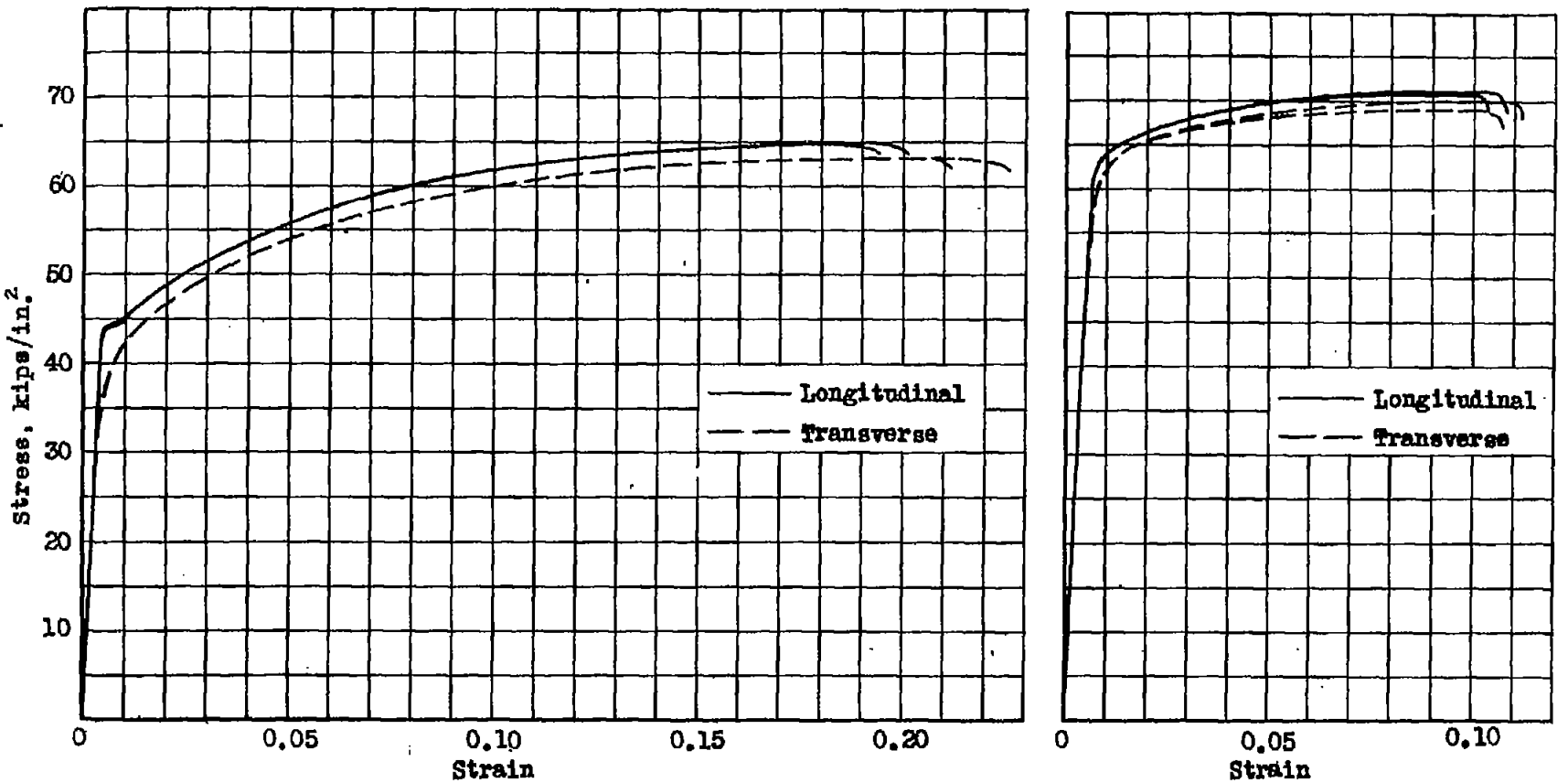

Aluminum alloy R301-W

Spec. no.	Tensile strength kips/in.^{2}	Elongation in 2 in. percent
T7L	64.8	19.0
T8L	65.0	19.5
T7T	63.3	21.8
T8T	63.3	20.5

Aluminum alloy R301-T

Spec. no.	Tensile strength kips/in.^{2}	Elongation in 2 in. percent
T7L	70.7	9.8
T8L	71.2	10.3
T7T	69.1	10.4
T8T	70.1	10.6

Figure 35. Tensile stress-strain curves to failure, thickness of sheet 0.032 in.

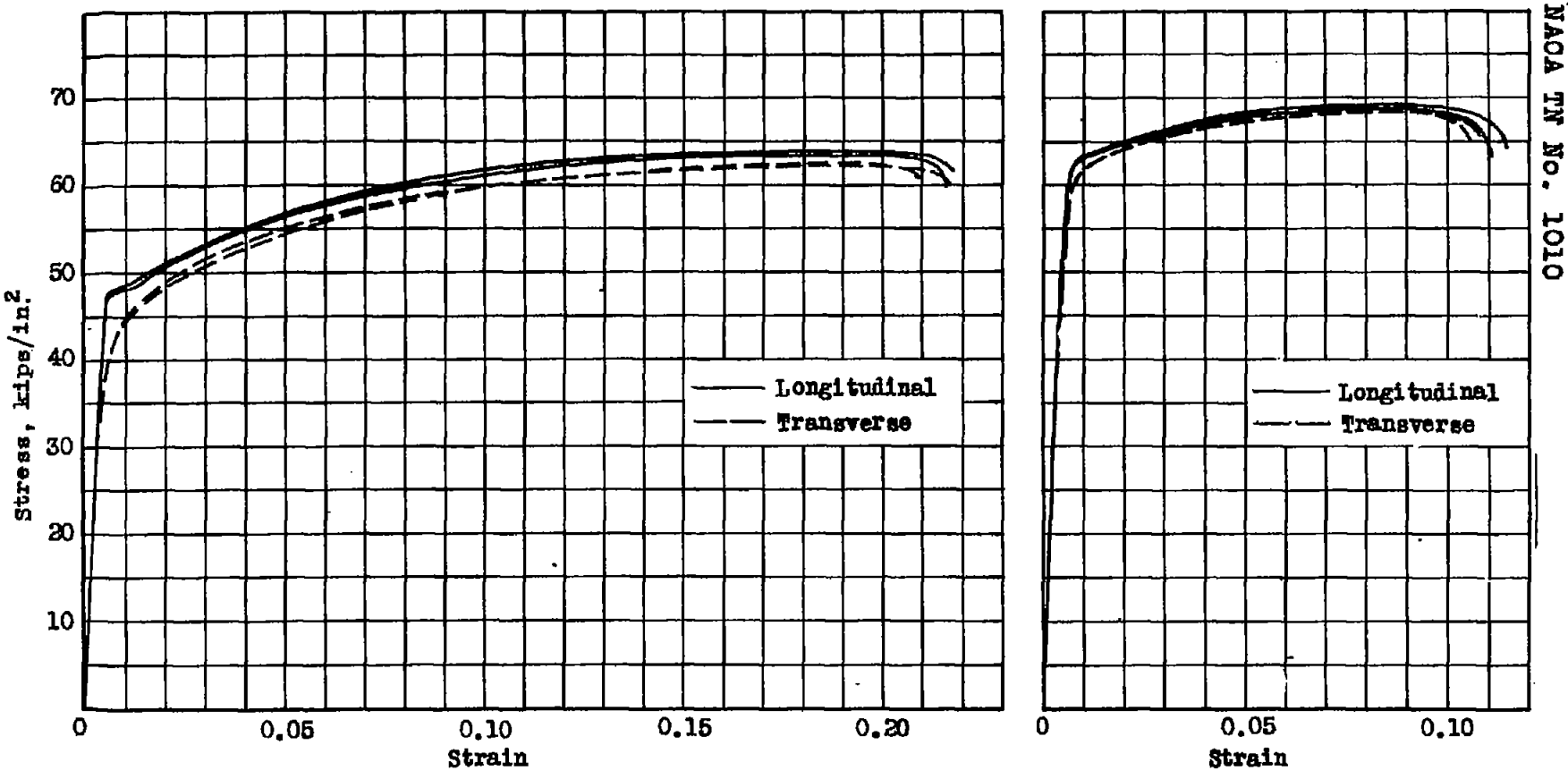

Aluminum alloy R301-W

Spec. no.	Tensile strength kips/in.^{2}	Elongation in 2 in. percent
T7L	63.5	20.8
T8L	64.1	21.3
T7T	62.2	21.2
T8T	62.5	20.2

Aluminum alloy R301-T

Spec. no.	Tensile strength kips/in.^{2}	Elongation in 2 in. percent
T7L	69.3	10.8
T8L	68.8	10.4
T7T	68.4	10.4
T8T	68.3	10.1

Figure 36. Tensile stress-strain curves to failure, thickness of sheet 0.064 in.

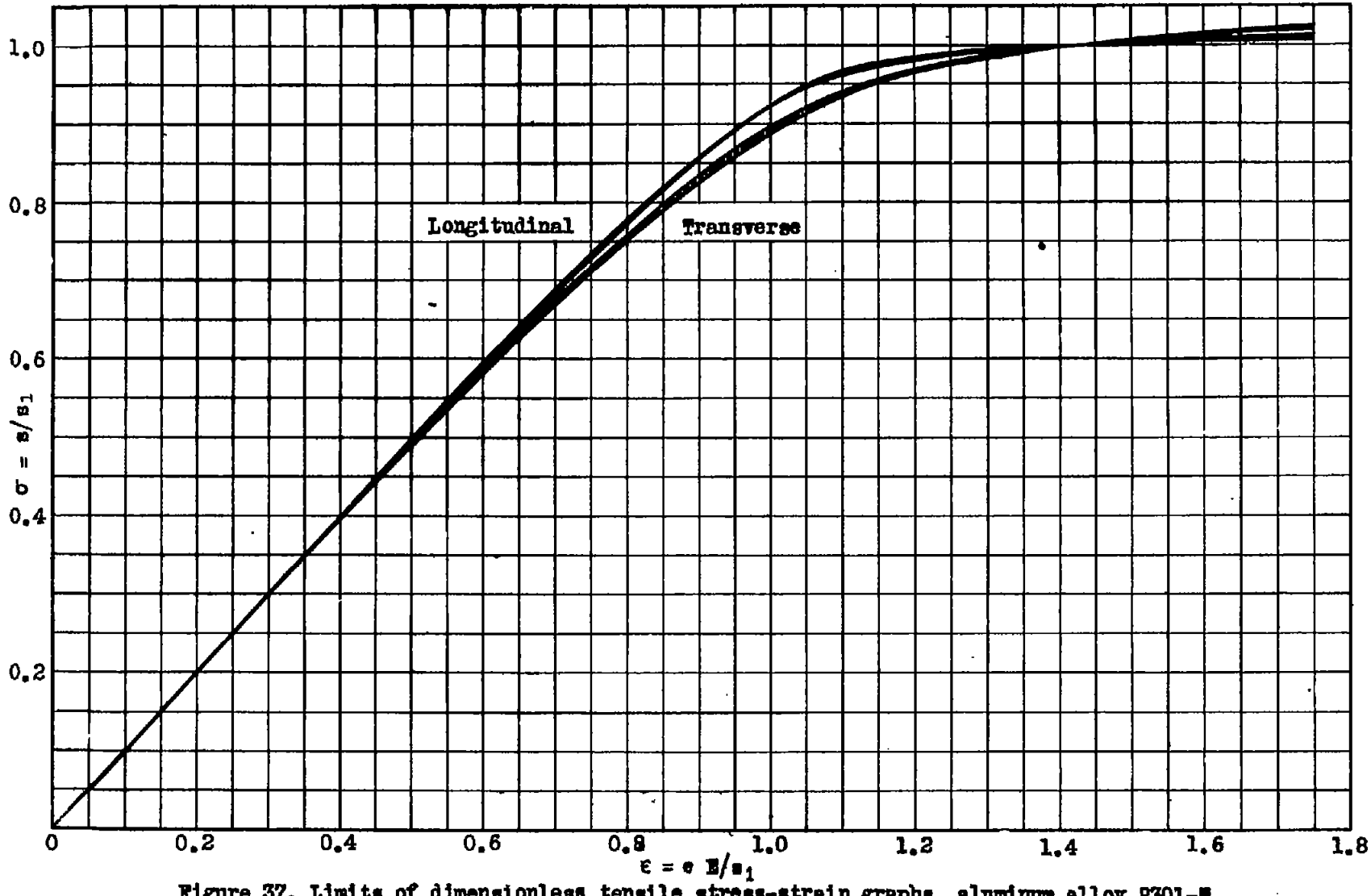

Figure 37. Limits of dimensionless tensile stress-strain graphs, aluminum alloy R301-T sheets 0.020, 0.032 and 0.064 in. thick.

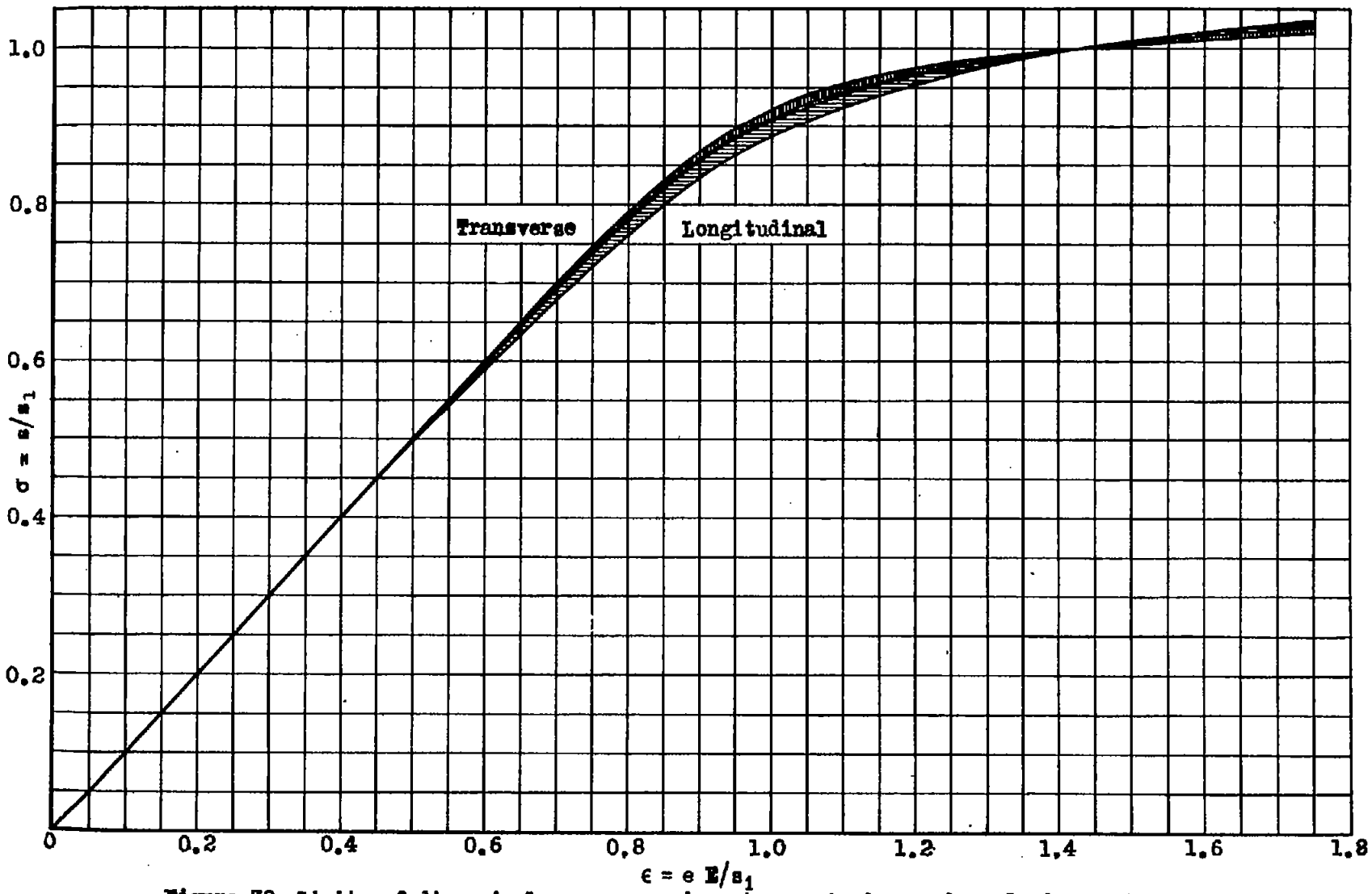

Figure 38. Limits of dimensionless compressive stress-strain graphs, aluminum alloy R301-T sheets 0.020, 0.032 and 0.064 in. thick.

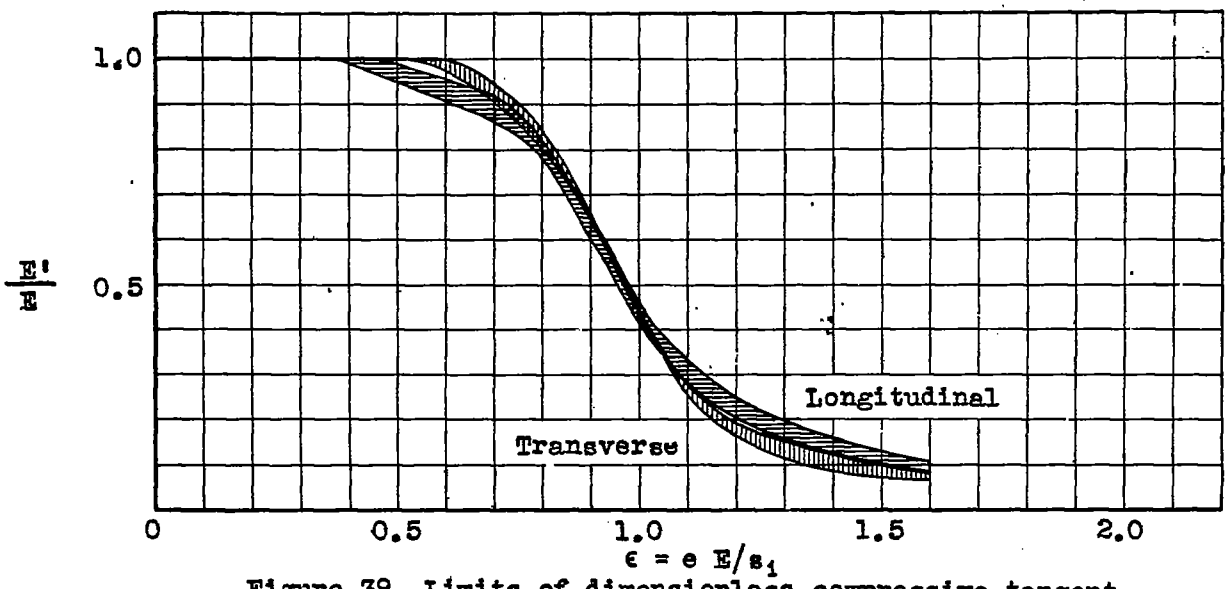

Figure 39. Limits of dimensionless compressive tangent-modulus-strain graphs, aluminum alloy R301-T sheets 0.020, 0.032 and 0.064 in. thick.

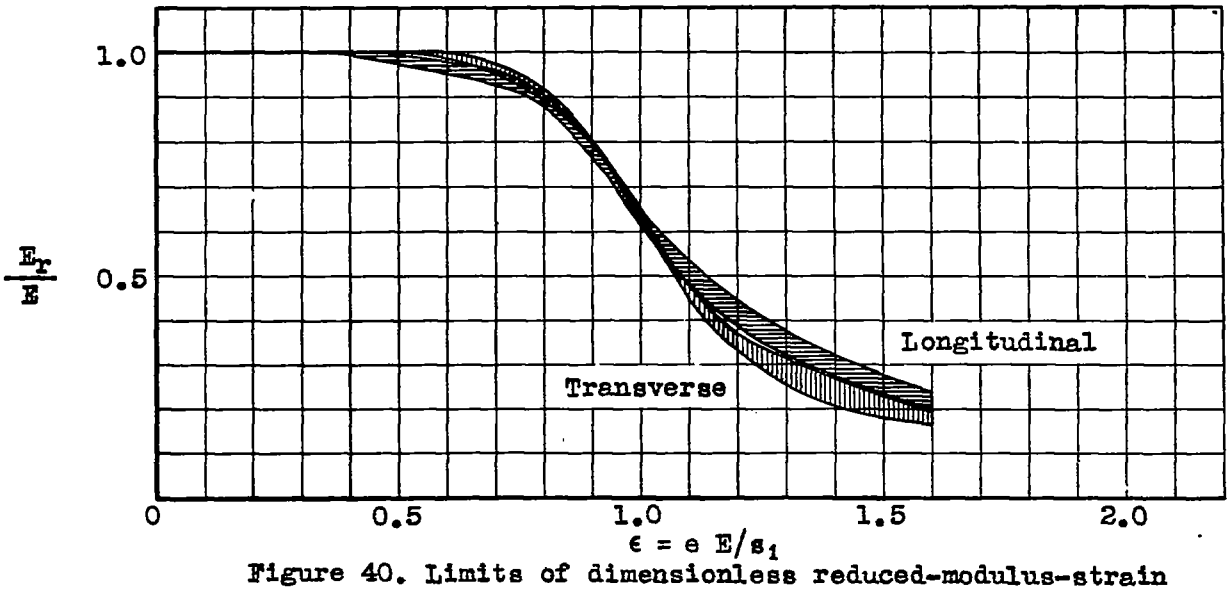

Figure 40. Limits of dimensionless reduced-modulus-strain graphs for rectangular sections, aluminum alloy R301-T sheets 0.020, 0.032 and 0.064 in. thick.